cifically from Der p1, Der p3, and Der p9, which may activate protease-activated receptor-2 in human keratinocytes.[38,39] A recent report has shown that activation of protease-activated receptor-2 through Dp application significantly delays barrier recovery rate in barrier function-perturbed skin or compromised skin.[39] Therefore, Dp may play a dual role in the onset of AD, both as an allergen and proteolytic signal and as a perturbation factor of the barrier function, leading to the persistence of eczematous skin lesions in AD.[39,40]

To address the issue of variable genetic background, we observed immune responses in mice of other genotypes, such as BALB/c and C3H, as controls, but both of these lines exhibited much less severe CHS responses compared with those in *Flg*[ft] mice (data not shown), suggesting that the enhanced immune responses seen in *Flg*[ft] mice were not solely due to their genetic background. The effect of the *ma* mutation in relation to the *ft* mutation in commercially available *Flg*[ft] mice in the development of AD-like skin lesions needs to be clarified in future studies. Furthermore, our study showed that heterozygous mice intercrossed with *Flg*[ft] mice and B6 mice did not develop spontaneous dermatitis. In this way they are unlike human AD patients, most of whom are heterozygous for the *FLG* mutation. Not only human studies but also additional mouse studies are required to clarify these relationships.

In this study, we have shown that *Flg*[ft] mice exhibit spontaneous dermatitis resembling human AD, enhanced irritation dermatitis and a contact hypersensitivity response, and mite-induced AD-like skin lesions, which provide hints for possible mechanisms in the human disease. These results suggest that *Flg*[ft] mice have the potential to serve as an animal model of human AD and further accentuate the important role of filaggrin in skin barrier function in the pathogenesis of AD.

References

1. Jin H, He R, Oyoshi M, Geha RS: Animal models of atopic dermatitis. J Invest Dermatol 2009, 129:31–40
2. Wollenberg A, Bieber T: Atopic dermatitis: from the genes to skin lesions. Allergy 2000, 55:205–213
3. Novak N, Bieber T, Leung DY: Immune mechanism leading to atopic dermatitis. J Allergy Clin Immunol 2003, 112:S128–S139
4. Elias PM, Hatano Y, Williams ML: Basis for the barrier abnormality in atopic dermatitis: outside-inside-outside pathogenic mechanism. J Allergy Clin Immunol 2008, 121:1337–1343
5. Palmer CN, Irvine AD, Terron-Kwiatkowski A, Zhao Y, Liao H, Lee SP, Goudie DR, Sandilands A, Campbell LE, Smith FJ, O'Regan GM, Watson RM, Cecil JE, Bale SJ, Compton JG, DiGiovanna JJ, Fleckman P, Lewis-Jones S, Arseculeratne G, Sergeant A, Munro CS, El Houate B, McElreavey K, Halkjaer LB, Bisgaard H, Mukhopadhyay S, McLean WH: Common loss-of function variants of the epidermal barrier protein filaggrin are a major predisposing factor for atopic dermatitis. Nat Genet 2006, 38:441–446
6. Nomura T, Sandilands A, Akiyama M, Liao H, Evans AT, Sakai K, Ota M, Sugiura H, Yamamoto K, Sato H, Palmer CN, Smith FJ, McLean WH, Shimizu H: Unique mutations in the filaggrin gene in Japanese patients with ichthyosis vulgaris and atopic dermatitis. J Allergy Clin Immunol 2007, 119:434–440
7. Morar N, Cookson WO, Harper JI, Moffat MF: Filaggrin mutations in children with severe atopic dermatitis. J Invest Dermatol 2007, 127:1667–1672
8. Dale BA: Filaggrin, the matrix protein of keratin. Am J Dermatopathol 1985, 7:65–68
9. Listwan P, Rothnagel JA: Keratin bundling proteins. Methods Cell Biol 2004, 78:817–827
10. Candi E, Schmidt R, Melino G: The cornified envelope: a model of cell death in the skin. Nat Rev Mol Cell Biol 2005, 6:328–340
11. Gan SQ, McBride OW, Idler WW, Markova N, Steinert RM: Organization, structure, and polymorphisms of the human profilaggrin gene. Biochemistry 1990, 29:9432–9440
12. Shiohara T, Hayakawa J, Mizukawa Y: Animal models for atopic dermatitis: are they relevant to human disease? J Dermatol Sci 2004, 36:1–9
13. Lane P: Two new mutations in linkage group XVI of the house mouse. J Hered 1972, 63:135–140
14. Presland RB, Boggess D, Lewis SP, Hull C, Fleckman P, Sundberg JP: Loss of normal profilaggrin and filaggrin in flaky tail (ft/ft) mice: an animal model for the filaggrin-deficient skin disease ichthyosis vulgaris. J Invest Dermatol 2000, 115:1072–1081
15. Fallon PG, Sasaki T, Sandilands A, Campbell LE, Saunders SP, Mangan NE, Callanan JJ, Kawasaki H, Shiohama A, Kubo A, Sundberg JP, Presland RB, Fleckman P, Shimizu N, Kudoh J, Irvine AD, Amagai M, McLean WH: A homozygous frameshift mutation in the mouse Flg gene facilitates enhanced percutaneous allergen priming. Nat Genet 2009, 41:602–608
16. Scharschmidt TC, Man MQ, Hatano Y, Crumrine D, Gunathilake R, Sundberg JP, Silva KA, Mauro TM, Hupe M, Cho S, Wu Y, Celli A, Schmuth M, Feingold KR, Elias PM: Filaggrin deficiency confers a paracellular barrier abnormality that reduces inflammatory thresholds to irritants and haptens. J Allergy Clin Immunol 2009, 124:496–506, 506.e1–e6
17. Oyoshi MK, Murphy GF, Geha RS: Filaggrin-deficient mice exhibit Th17-dominated skin inflammation and permissiveness to epicutaneous sensitization with protein antigen. J Allergy Clin Immunol 2009, 124:475–493, 493.e1
18. Leung DY, Hirsch RL, Schneider L, Moody C, Takaoka R, Li SH, Meyerson LA, Mariam SG, Goldstein G, Hanifin JM: Thymopentin therapy reduces the clinical severity of atopic dermatitis. J Allergy Clin Immunol 1990, 85:927–933
19. Mori T, Kabashima K, Yoshiki R, Sugita K, Shiraishi N, Onoue A, Kuroda E, Kobayashi M, Yamashita U, Tokura Y: Cutaneous hypersensitivities to hapten are controlled by IFN-γ-upregulated keratinocyte Th1 chemokines and IFN-γ-downregulated Langerhans cell Th2 chemokines. J Invest Dermatol 2008, 128:1719–1727
20. Orito K, Chida Y, Fujisawa C, Arkwright PD, Matsuda H: A new analytical system for quantification scratching behavior in mice. Br J Dermatol 2004, 150:33–38
21. Gupta J, Grube E, Ericksen MB, Stevenson MD, Lucky AW, Sheth AP, Assa'ad AH, Khurana Hershey GK: Intrinsically defective skin barrier function in children with atopic dermatitis correlates with disease severity. J Allergy Clin Immunol 2008, 121:725–730
22. Novak N: New insights into the mechanism and management of allergic diseases: atopic dermatitis. Allergy 2009, 64:265–275
23. Kang JS, Lee K, Han SB, Ahn JM, Lee H, Han MH, Yoon YD, Yoon WK, Park SK, Kim HM: Induction of atopic eczema/dermatitis syndrome-like skin lesions by repeated topical application of a crude extract of Dermatophagoides pteronyssinus in NC/Nga mice. Int Immunopharmacol 2006, 6:1616–1622
24. Yamamoto M, Haruna T, Yasui K, Takahashi H, Iduhara M, Takaki S, Deguchi M, Arimura A: A novel atopic dermatitis model induced by topical application with Dermatophagoides farinae extract in NC/Nga mice. Allergol Int 2007, 56:139–148
25. Matsumoto M, Ra C, Kawamoto K, Sato H, Itakura A, Sawada J, Ushio H, Suto H, Mitsuishi K, Hikasa Y, Matsuda H: IgE hyperproduction through enhanced tyrosine phosphorylation of Janus kinase 3 in NC/Nga mice, a model for human atopic dermatitis. J Immunol 1999, 162:1056–1063
26. Cooper D, Hales J, Camp R: IgE-dependent activation of T cells by allergen in atopic dermatitis: pathophysiologic relevance. J Invest Dermatol 2004, 123:1086–1091
27. The International Study of Asthma and Allergies in Childhood (ISAAC) Steering Committee: Worldwide variation in prevalence of symptoms of asthma, allergic rhinoconjunctivitis, and atopic eczema: ISAAC. Lancet 1998, 351:1225–1232
28. Williams H, Robertson C, Stewart A, Aït-Khaled N, Anabwani G,

Anderson R, Asher I, Beasley R, Björkstén B, Burr M, Clayton T, Crane J, Ellwood P, Keil U, Lai C, Mallol J, Martinez F, Mitchell E, Montefort S, Pearce N, Shah J, Sibbald B, Strachan D, von Mutius E, Weiland S: Worldwide variations in the prevalence of symptoms of atopic eczema in the international study of asthma and allergies in childhood. J Allergy Clin Immunol 1999, 103:125–138

29. Nemoto-Hasebe I, Akiyama M, Nomura T, Sandilands A, McLean WHI, Shimizu H: Clinical severity correlates with impaired barrier in filaggrin-related eczema. J Invest Dermatol 2009, 129:682–689

30. Willis CM, Shaw S, De Lacharrière O, Baverel M, Reiche L, Jourdain R, Bastien P, Wilkinson JD: Sensitive skin: an epidemiological study. Br J Dermatol 2001, 145:258–263

31. Farage MA, Katsarou A, Maibach HI: Sensory, clinical and physiological factors in sensitive skin: a review. Contact Dermatitis 2006, 55:1–14

32. Clayton TH, Wilkinson SM, Rawcliffe C, Pollock B, Clark SM: Allergic contact dermatitis in children: should pattern of dermatitis determine referral? A retrospective study of 500 children tested between 1995 and 2004 in one UK centre. Br J Dermatol 2006, 154:114–117

33. Mailhol C, Lauwers-Cances V, Rance F, Paul C, Giordano-Labadie F: Prevalence and risk factors for allergic contact dermatitis to topical treatment in atopic dermatitis: a study in 641 children. Allergy 2009, 64:801–806

34. Yilmaz M, Bingöl G, Altintas D, Kendirli SG: Correlation between atopic diseases and tuberculin responses. Allergy 2000, 55:664–667

35. Grüber C, Kulig M, Bergmann R, Guggenmoos-Holzmann I, Wahn U, MAS-90 Study Group: Delayed hypersensitivity to tuberculin, total immunoglobulin E, specific sensitization, and atopic manifestation in longitudinally followed early Bacille Calmette-Guérin-vaccinated and nonvaccinated children. Pediatrics 2001, 107:e36

36. Kimura M, Tsuruta S, Yoshida T: Correlation of house dust mite-specific lymphocyte proliferation with IL-5 production, eosinophilia, and the severity of symptoms in infants with atopic dermatitis. J Allergy Clin Immunol 1998, 101:85–89

37. Henderson J, Northstone K, Lee SP, Liao H, Zhao Y, Pembrey M, Mukhopadhyay S, Smith GD, Palmer CN, McLean WH, Irvine AD: The burden of disease associated with filaggrin mutations: a population-based, longitudinal birth cohort study. J Allergy Clin Immunol 2008, 121:872–877

38. Vasilopoulos Y, Cork MJ, Teare D, Marinou I, Ward SJ, Duff GW, Tazi-Ahnini R: A nonsynonymous substitution of cystatin A, a cysteine protease inhibitor of house dust mite protease, leads to decreased mRNA stability and shows a significant association with atopic dermatitis. Allergy 2007, 62:514–519

39. Jeong SK, Kim HJ, Youm JK, Ahn SK, Choi EH, Sohn MH, Kim KE, Hong JH, Shin DM, Lee SH: Mite and cockroach allergens activate protease-activated receptor 2 and delay epidermal permeability barrier recovery. J Invest Dermatol 2008, 128:1930–1939

40. Roelandt T, Heughebaert C, Hachem JP: Proteolytically active allergens cause barrier breakdown. J Invest Dermatol 2008, 128:1878–1880

blood

Rho-mDia1 pathway is required for adhesion, migration, and T-cell stimulation in dendritic cells

Hideaki Tanizaki, Gyohei Egawa, Kayo Inaba, Tetsuya Honda, Saeko Nakajima, Catharina Sagita Moniaga, Atsushi Otsuka, Toshimasa Ishizaki, Michio Tomura, Takeshi Watanabe, Yoshiki Miyachi, Shuh Narumiya, Takaharu Okada and Kenji Kabashima

Rho-mDia1 pathway is required for adhesion, migration, and T-cell stimulation in dendritic cells

Hideaki Tanizaki,[1] Gyohei Egawa,[1,2] Kayo Inaba,[3] Tetsuya Honda,[1] Saeko Nakajima,[1] Catharina Sagita Moniaga,[1] Atsushi Otsuka,[1] Toshimasa Ishizaki,[4] Michio Tomura,[5] Takeshi Watanabe,[2] Yoshiki Miyachi,[1] Shuh Narumiya,[4] Takaharu Okada,[6] and Kenji Kabashima[1,2]

[1]Department of Dermatology and [2]Center for Innovation in Immunoregulative Technology and Therapeutics, Kyoto University Graduate School of Medicine, Kyoto, Japan; [3]Department of Animal Development and Physiology, Kyoto University Graduate School of Biostudies, Kyoto, Japan; [4]Department of Pharmacology, Kyoto University Graduate School of Medicine, Kyoto, Japan; and [5]Laboratory for Autoimmune Regulation and [6]Research Unit for Immunodynamics, Research Center for Allergy & Immunology, RIKEN, Yokohama, Japan

Dendritic cells (DCs) are essential for the initiation of acquired immune responses through antigen acquisition, migration, maturation, and T-cell stimulation. One of the critical mechanisms in this response is the process actin nucleation and polymerization, which is mediated by several groups of proteins, including mammalian Diaphanous-related formins (mDia). However, the role of mDia in DCs remains unknown. Herein, we examined the role of mDia1 (one of the isoforms of mDia) in DCs. Although the proliferation and maturation of bone marrow-derived DCs were comparable between control C57BL/6 and mDia1-deficient (mDia1$^{-/-}$) mice, adhesion and spreading to cellular matrix were impaired in mDia1$^{-/-}$ bone marrow-derived DCs. In addition, fluorescein isothiocyanate-induced cutaneous DC migration to draining lymph nodes in vivo and invasive migration and directional migration to CCL21 in vitro were suppressed in mDia1$^{-/-}$ DCs. Moreover, sustained T-cell interaction and T-cell stimulation in lymph nodes were impaired by mDia1 deficiency. Consistent with this, the DC-dependent delayed hypersensitivity response was attenuated by mDia1-deficient DCs. These results suggest that actin polymerization, which is mediated by mDia1, is essential for several aspects of DC-initiated acquired immune responses. (*Blood*. 2010;116(26):5875-5884)

Introduction

When external antigens invade the body, professional antigen-presenting dendritic cells (DCs) capture them, up-regulate the expression levels of costimulatory molecules and chemokine receptors such as CCR7 and CXCR4, and migrate to draining lymphoid tissues via the lymphatic vessels.[1-4] During the initial phase of T-cell priming within the T-cell areas of lymph nodes (LNs), DCs project polarized membrane extensions that facilitate repeated and, under certain conditions, sustained DC-T cell contacts called immunologic synapses, which facilitate T-cell proliferation and differentiation.[5]

The actin cytoskeleton undergoes continuous remodeling and serves as the machinery for antigen acquisition, cell migration, and sustained cell contact.[6-8] A critical step in this remodeling process is the formation of actin oligomers, which serve as nuclei for further polymerization. Actin nucleation and polymerization in mammalian cells are catalyzed by several groups of proteins. Two of the most important catalyst groups here are the mammalian Diaphanous-related (mDia) formins, which produce long and straight actin filaments, and the Wiskott-Aldrich syndrome protein (WASP)–Arp2/3 system, which produces a branched actin meshwork.[9] Lack of WASP expression results in defects in T-cell proliferation, T-cell receptor capping, phagocytosis of macrophages, and migration of immune cells,[10] all of which are involved in chemotaxis, chemokinesis, and adhesion.[11]

The mDia family formins are among the effectors of Rho GTPase. The family is composed of 3 isoforms: mDia1, mDia2, and mDia3. The ability of mDia proteins to promote rapid assembly of actin filaments appears to be crucial to cell polarity, morphogenesis, and cytokinesis.[12-15] Most studies on the mDia family have used cultured cells.[9] As a result, the roles of mDia proteins in vivo remain unclear. Recently, we and other researchers have generated mice deficient in mDia1 and reported on its role in T-cell proliferation, trafficking, and interaction with DCs.[16,17]

Because the mDia family drives actin polymerization, mDia proteins may contribute to the functions of DCs,[18] but the roles of mDia in DCs are still unclear. In this study, we studied mDia1-deficient (mDia1$^{-/-}$) mice and the cells derived from these mice, and found that mDia1 in DCs is essential for adhesion to fibronectin, transmigration through small pore membranes, directional migration, and sustained interaction with T cells.

Methods

Mice, reagents, flow cytometry, and cell sorting

We generated mDia1$^{-/-}$ mice[16] and backcrossed them for more than 10 generations onto C57BL/6J Slc (B6) mice (Japan SLC Inc). OT-I, OT-II (The Jackson Laboratory), and BALB/c (Japan SLC Inc) mice were bred at the Institute of Laboratory Animals at Kyoto University on a 12-hour

light/dark cycle under specific pathogen–free conditions. Eight- to 10-week-old female mice were used for all experiments. All experimental procedures were approved by the Institutional Animal Care and Use Committee of Kyoto University Graduate School of Medicine.

Carboxyfluorescein succinimidyl ester (CFSE) and CellTracker Red CMTPX were purchased from Invitrogen. Fluorescein isothiocyanate (FITC), phycoerythrin (PE), PE-Cy5, PE-Cy7, allophycocyanin, Pacific Blue–conjugated RM4-5 (anti-CD4), 53-6.7 (anti-CD8), HI111 (anti-CD11a), M1/70 (anti-CD11b), HL3 (anti-CD11c), HM40-3 (anti-CD40), YN1/1.7.4 (anti-CD54), Ly-22 (anti-CD62L), 16-10A1 (anti-CD80), 24-31 (anti-OX40L), GL1 (anti-CD86), M5/114.15.2 (anti–major histocompatibility complex [MHC] class II), 4B12 (anti-CCR7) monoclonal antibodies (Abs), and PE-Cy7–conjugated streptavidin were purchased from eBioscience. Biotin-conjugated eBioRMUL2 (anti-Langerin) and PECy-7–conjugated H1.2F3 (anti-CD69) Abs were purchased from BD Biosciences. Flow cytometry was performed using FACSCanto II (BD Biosciences) and analyzed with FlowJo Version 8.8.7 software (TreeStar). Cell sorting was performed using an autoMACS system (Miltenyi Biotec) or a cell sorter (FACSAria II, BD Biosciences).[19]

Cell culture, MLR, and enzyme-linked immunosorbent assay

The complete RPMI (cRPMI) culture medium consisting of RPMI 1640 (Sigma-Aldrich) containing 10% heat-inactivated fetal calf serum, 5×10^{-5}M 2-mercaptoethanol, 2mM L-glutamine, 25mM N-2-hydroxyethylpiperazine-N'-2-ethanesulfonic acid, 1mM nonessential amino acids, 1mM sodium pyruvate, 100 units/mL penicillin, and 100 μg/mL streptomycin, was used, unless otherwise indicated.

For bone marrow–derived DC (BMDC) culture, 5×10^6 BM cells were cultured in 10 mL of cRPMI supplemented with 5 ng/mL recombinant murine granulocyte-macrophage colony-stimulating factor (PeproTech) for 5 to 7 days.[20]

For spleen cell suspensions, spleens were cut into small pieces and digested by being mixed for 25 minutes at 37°C with RPMI 1640 containing 1.6 mg/mL type II collagenase (Worthington Biochemical) and 100 μg/mL DNase I (Sigma-Aldrich).

For epidermal cell suspensions, ear skin sheets were floated on 0.25% trypsin in phosphate-buffered saline (PBS) for 30 minutes at 37°C.[21] The epidermis was separated from the dermis with forceps in PBS supplemented with 10% fetal calf serum. The epidermis was filtered through a 40-μm cell strainer. For dermal cell suspensions, the dermis was further digested with 1.6 mg/mL type II collagenase and 100 μg/mL DNase I in cRPMI for 25 minutes at 37°C. The cells were then filtered through a 40-μm cell strainer.

For allogeneic mixed lymphocyte reaction (MLR), 1×10^3 or 10^4 BMDCs with a B6 background were pretreated with mitomycin C and incubated with 5×10^5 CD4+ T cells from BALB/c mice in 200 μL of cRPMI for 3 days. The cells were pulsed with 0.5 μCi ³H-thymidine for the last 24 hours and subjected to liquid scintillation counting. For the measurement of cytokine production, culture supernatants were collected 72 hours after the start of cultivation and measured with an enzyme-linked immunosorbent assay kit (BD Biosciences).

Chemotaxis, TAXIScan, adhesion, cell polarity, and FITC-induced DC migration assays

For the chemotaxis assay, suspensions of epidermal cells were prepared and incubated overnight, then 1×10^6 cells were transferred into the upper chamber of the transwell with 3- or 8-μm pore size filters (BD Biosciences), and 10 or 100 ng/mL of CCL21 (R&D Systems) was added to the lower chamber and allowed to incubate for 3 hours or 24 hours at 37°C. The cells that migrated to the lower chambers were stained with MHC class II and counted by flow cytometry. The migration index was presented as a percentage of input: the number of cells in each lower chamber was divided by the total number of cells placed in the corresponding upper chamber.

For the evaluation of invasive migration, the upper chambers (8-μm pore size) were coated with Matrigel (BD Biosciences), which consists of laminin, collagen IV, heparin sulfate proteoglycans, and entactin/nidogen. After 24 hours of incubation, the upper chambers were washed 3 times with

500 μL of PBS. The upper chambers were treated with 500 μL of dispase (0.15 mg/mL; Invitrogen), cRPMI for 60 minutes at 37°C to collect the cells in the Matrigel.

For the TAXIScan assay, time-lapse images of BMDCs during chemotaxis were obtained using TAXIScan (GE Healthcare) as described previously.[22] First, 2×10^6 BMDCs were applied to the lower side of the chamber. Data were collected at 60-second intervals for 6 hours, starting at 10 minutes after addition of 1 μL of CCL21 (10 μg/mL) to the upper side of the chamber, and analyzed with the TAXIScan Analyzer 2 (GE Healthcare).

For the adhesion assay, 4×10^4 CFSE-labeled BMDCs were incubated in a 96-well plate that had previously been coated overnight with PBS with or without 10 μg/mL of fibronectin (FN), and incubated for 45 minutes at 37°C. The plate was read in a fluorescent plate reader (Wallac 1420 ARVOsx, PerkinElmer Life and Analytical Sciences) at 485-nm excitation and 535-nm emission, both immediately after incubation, to determine the original number of cells (the fluorescent total). The plate was read again after it had been washed twice by vigorous pipetting with 200 μL of PBS and decanting, to determine the number of cells that had adhered (the fluorescent adhesion). The percentage of adherence was calculated as the ratio of fluorescent adhesion/fluorescent total.

To evaluate the cell polarity induced by the chemokine gradient, 25 μL of CCL21 (10 ng/mL) was added to the edge of the BMDC culture in 24-well plates. Thirty minutes later, the culture medium was washed out, and the cells were fixed, permeabilized, and stained with phalloidin.

For FITC-induced cutaneous DC migration, the footpads of mice were painted with 50 μL of 2% FITC (Sigma-Aldrich), dissolved in a 1:1 (vol/vol) acetone/dibutyl phthalate (Sigma-Aldrich) mixture; 72 hours later, the number of cutaneous DCs that had migrated into skin-draining popliteal and inguinal LNs was counted by flow cytometry.

Immunostaining

BMDCs were plated on coverslips coated with or without 10 μg/mL FN for 16 hours. The cells were fixed for 15 minutes with 3.7% formalin (Wako) and permeabilized with 0.1% Triton-X (Sigma-Aldrich) in PBS for 7 minutes at room temperature. Next, slides were incubated with the anti-mDia1 or anti-vinculin Ab (BD Biosciences) and Alexa Fluor 488–conjugated phalloidin (Invitrogen) at room temperature for 1 hour, then stained with Alexa Fluor 546–conjugated goat anti–mouse IgG (Invitrogen) for 30 minutes at room temperature. The slides were mounted in ProLong Gold Antifade reagent (Invitrogen), and fluorescence images were obtained using a BIOREVO BZ-9000 system (Keyence).

Antigen acquisition, DC kinetics, T-cell priming, and DTH model

The activity of antigen acquisition by DCs was measured with 2 mg/mL FITC-ovalbumin (OVA; Invitrogen). After incubation for 45 minutes at 4°C or 37°C, the cells were washed 4 times with PBS and the mean fluorescence intensity of FITC was measured by flow cytometry.[22]

For the evaluation of the kinetics of DCs in the LNs, BMDCs were cultured for 7 days, stimulated with 200 ng/mL of lipopolysaccharide (LPS) for 2 hours, and labeled with 5μM CFSE or 3.3μM CMTPX at 37°C for 20 minutes.

For the assessment of the interaction between CD4+ T cells and BMDCs, BMDCs were cultured for 7 days, pulsed with 1 μg/mL of OVA (Sigma-Aldrich) for 30 minutes at 37°C, stimulated with 200 ng/mL of LPS for 2 hours, and labeled with 5μM CFSE at 37°C for 20 minutes. A total of 3 million B6 or mDia1⁻/⁻ BMDCs were injected into the footpads of B6 mice. Twenty-four hours later, CD4+ T cells from OT-II mice purified with CD4+ T cell–negative separation kits (Miltenyi Biotec) were labeled with 3.3μM CMTPX and transferred into B6 mice intravenously (1×10^7 cells per mouse). Two hours later, the popliteal and inguinal LNs were harvested and observed for 90 minutes under 2-photon microscopy to measure the period of conjugate formation between T cells and DCs.

For assessing the ability of DCs to induce OT-II CD4+ T-cell proliferation or OT-I CD8+ T-cell proliferation, 20 μL of 0.5 μg/mL OVA emulsified with complete Freund adjuvant (CFA; Difco) and PBS (1:1) was injected into mouse footpads. CD4+ T cells from OT-II mice and CD8+ T cells from OT-I mice were isolated using magnetic bead separation

(Miltenyi Biotec) and labeled with 8μM CFSE. One day after injection of OVA-CFA emulsion, 1×10^7 CFSE-labeled OT-II CD4$^+$ T cells or OT-I CD8$^+$ T cells were transferred via the tail vein. After 48 hours, draining popliteal and inguinal LNs and nondraining axillary LNs were collected and analyzed by flow cytometry.

For delayed-type hypersensitivity (DTH) response, mice were sensitized with 20 μL of 0.5 mg/mL OVA in CFA or with 5×10^5 LPS-pretreated and 1-μg/mL-OVA-pulsed BMDCs in 20 μL PBS subcutaneously injected into the front footpads. Five days later, the mice were challenged with an injection of 20 μL of 0.5 mg/mL OVA in CFA into the hind footpads. Footpad swelling was measured before and 48 hours after the challenge. Controls consisted of CFA injections containing no OVA or sensitization with non–OVA-pulsed DCs.

Two-photon imaging

Two-photon imaging was performed as previously described[23] with some modifications. Briefly, we used a custom-built, video-rate multiphoton microscope: an upright BX61WI microscope (Olympus) fitted with a ×20 water-immersion objective lens (numerical aperture, 0.95), a Spectra-Physics Mai Tai femtosecond laser (Newport), and a resonant-mirror scan head. The image acquisition process, the z-axis stepper, shutters, and the emission filter wheel were under software control (FluoView10-ASW1.6, Olympus). LNs were cemented to the base of the imaging chamber with a thin film of veterinary-grade superglue and were continuously superperfused with warm (35°-37°C) RPMI 1640 medium bubbled with 95% O_2/5% CO_2.

Quantitative reverse-transcribed polymerase chain reaction analysis

Total RNA was isolated using an RNeasy kit (QIAGEN) with an on-column DNase I digestion kit (QIAGEN). cDNA was synthesized using the Prime Script RT reagent kit (Takara Bio). Quantitative polymerase chain reaction analysis was carried out with a Light Cycler 480 (Roche Diagnostics) using SYBR Green I (Takara Bio) with 40 cycles of 5 seconds at 95°C, 15 seconds at 60°C, and 10 seconds at 72°C. Primer sequences used in this study are as follows: *mDia1*, 5′-CGA CGG CGG CAA ACA TAA G-3′ (forward) and 5′-TGC AGA GGA GTT TCT ATG AGC A-3′ (reverse); *mDia2*, 5′-GAG AAG CGA CCC AAG TTG CAT-3′ (forward) and 5′-GAA GGG GAG GTC TCT CTT TCT T-3′ (reverse); *mDia3*, 5′-AAT CTT CTG GAA GCC CTA CAG T-3′ (forward) and 5′-GGC CGT CTG TTA TCT GGA TTT C-3′ (reverse); *Gapdh*, 5′-AAA CCC ATC ACC ATC TTC CA-3′ (forward) and 5′-GTG GTT CAC ACC CAT CAC AA-3′ (reverse). The reaction protocol included preincubation at 95°C to activate FastStart DNA polymerase for 1 minute, 40 cycles of amplification each consisting of 5 seconds at 95°C, annealing for 15 seconds at 60°C, and elongation for 10 seconds at 72°C. Relative quantification was performed after determining the cycle threshold (C_t) values for reference gene *Gapdh*, and target genes in each sample sets according to the $2-\Delta\Delta C_t$ method.[24] We verified that all primer sets used in this study showed similar amplification efficiency. For each sample, triplicate test reactions and a control reaction lacking reverse transcriptase were used.

Statistical analysis

Unless otherwise indicated, data are presented as mean plus or minus SD. *P* values were calculated with the 2-tailed Student *t* test after data were confirmed to meet the criteria of normal distribution and equal variance using Lilliefors test.

Results

mRNA expression of the mDia family in DCs

We examined expression of mRNA for the mDia isoforms in DCs through a quantitative reverse-transcribed polymerase chain reaction analysis. We prepared B6 and mDia1$^{-/-}$ BMDCs, epidermal
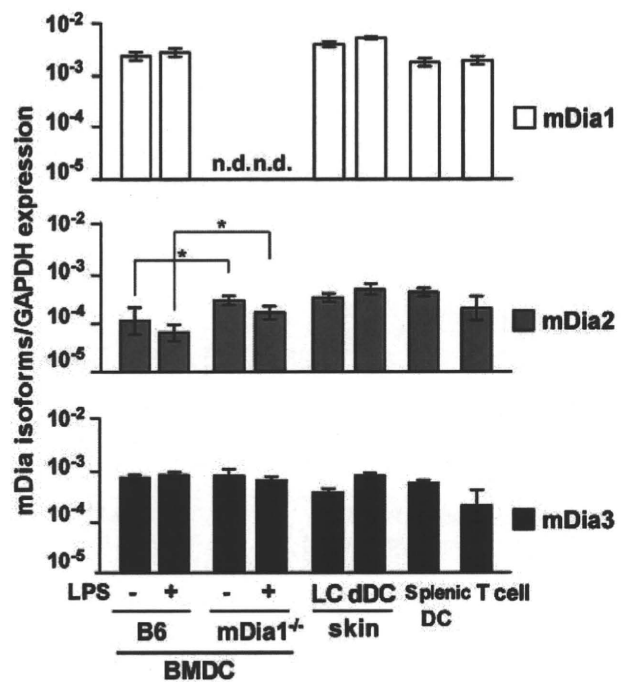

Figure 1. mRNA expression profiles of mDia isoforms in DCs. The mRNA expression profiles of mDia isoforms, mDia1, mDia2, and mDia3, in BMDCs from B6 and mDia1$^{-/-}$ mice stimulated with (+) or without (−) LPS, and LCs, dermal DCs, splenic DCs, and CD4$^+$ T cells from B6 mice. Data are expressed as the amounts of mRNA relative to that of glyceraldehyde-3-phosphate dehydrogenase (GAPDH). Data are mean ± SD (n = 3) of 3 independent experiments. n.d. indicates not dectected. *$P < .05$ vs corresponding B6 mice.

Langerhans cells (LCs), dermal and splenic DCs, and CD4$^+$ T cells of B6 mice and found that transcripts encoding all 3 isoforms were detected in all DC populations (Figure 1). The expression levels of the mDia isoforms in BMDCs were not affected by the maturation stimulated by LPS. In BMDCs from mDia1$^{-/-}$ mice, mDia1 expression was not detected as expected; and interestingly, mDia2 mRNA levels were higher than those of WT mice.

Impaired interstitial migration of cutaneous DCs in mDia1$^{-/-}$ mice

Initially, we evaluated the role of mDia1 in the development of DCs. The numbers of skin-derived DCs, resident DC subsets, splenic DC subsets, and skin DC subsets, and the maturation status of DCs in skin-draining LNs were comparable between B6 and mDia1$^{-/-}$ mice (supplemental Figure 1, available on the *Blood* Web site; see the Supplemental Materials link at the top of the online article). In addition, the number and maturation rates of mDia1$^{-/-}$ BMDCs were similar to those of B6 BMDCs in the absence (supplemental Figure 2A-D) or presence (supplemental Figure 2E) of 200 ng/mL LPS for the last 2 hours of 5-day cultivation period. These results suggest that mDia1 deficiency does not affect the development and maturation of conventional DCs.

We evaluated the significance of mDia1 with regard to DC functions in vivo. We used FITC, a fluorescent hapten, to induce DC maturation and mobilization.[25,26] FITC applied topically to the footpads of mice is taken up by cutaneous DCs, which then migrate to draining popliteal and inguinal LNs as MHC class II$^+$ FITC$^+$ cells.[27] The number of MHC class II$^+$ FITC$^+$ DCs that accumulated in draining LNs was significantly lower in mDia1$^{-/-}$ mice than in B6 mice (Figure 2A), and the numbers of Langerin$^+$ DCs (including both LCs and Langerin$^+$ dermal DCs) and Langerin$^-$
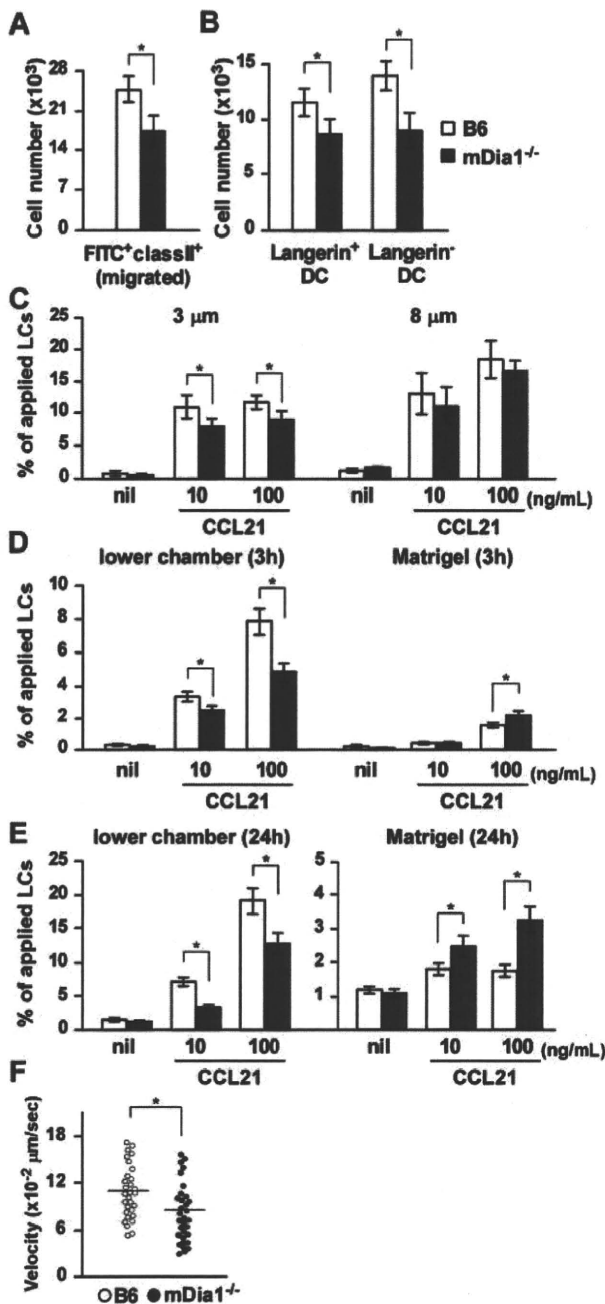
Figure 2. Impaired cutaneous DC migration in mDia1⁻/⁻ mice. (A) The number of cutaneous DCs migrating from the skin to draining LNs. The numbers of FITC⁺ MHC class II⁺ total DCs (A) and FITC⁺ MHC class II⁺ Langerin⁺ DC and FITC⁺ MHC class II⁻ Langerin⁻ DC subsets (B) in draining LNs of B6 (open bars) and mDia1⁻/⁻ mice (shaded bars) were analyzed 72 hours after application of FITC to the footpad. Bars represent the mean ± SD from at least 3 mice per group. (C) Mobility of LCs to CCL21. Epidermal cell suspensions were applied to the upper chamber of a transwell with 3 μm (left panel) and 8 μm (right panel) pore size without coating for 3 hours. Percentages of MHC class II⁺ LCs that migrated from the upper chambers to the lower are shown. (D-E) Invasive movement of LCs to CCL21. Epidermal cell suspensions were applied to the upper chamber of a transwell coated with Matrigel for 3 hours (D) and 24 hours (E). The numbers of MHC class II⁺ cells in the lower chamber (left panels) or in the Matrigel (right panels) were counted with flow cytometry. Data are mean ± SD of 3 independent experiments. *P < .05 vs corresponding B6 mice. (F) TAXIScan assay. BMDCs chemotaxing under the CCL21 gradient were analyzed with TAXIScan. BMDCs from B6 and mDia1⁻/⁻ mice were compared in terms of the velocity. Data are mean ± SD of 4 independent experiments. *P < .05 vs corresponding B6 mice.

dermal DCs among the FITC⁺ population of mDia1⁻/⁻ mice were lower in mDia1⁻/⁻ mice than in B6 mice (Figure 2B). On the other hand, FITC⁺ mDia1⁻/⁻ DCs were localized appropriately in the

T zone of draining LNs, as observed using fluorescent microscopy (data not shown).

To assess the role of mDia1 in DC mobility, we performed a transwell assay with 3- and 8-μm pore sizes. Epidermal cell suspensions from the ears of B6 and mDia1⁻/⁻ mice were applied to the upper transwell chambers, and the numbers of MHC class II⁺ LCs in lower chambers with or without CCL21 were measured. The chemotaxis of mDia1⁻/⁻ LCs to lower chambers containing CCL21 through the 8-μm transwell tended to be low, but not significantly so, compared with that of B6 LCs (Figure 2C right panel). The impaired chemotaxis of LCs by mDia1 deficiency became more distinct when transwells with a smaller pore size (3 μm) were used (Figure 2C left panel), suggesting that mDia1 is more essential to cell polarity-dependent transmigration. Next, we evaluated the invasion and directional movement of LCs by coating the polycarbonate filters of the 8-μm transwell with Matrigel.[28] Three hours after application, the number of LCs in the Matrigel was increased by the addition of CCL21 to the lower chamber, which was further increased by deficiency of mDia1 (Figure 2D right panel). On the other hand, the number of LCs in the lower chamber was decreased by deficiency of mDia1 (Figure 2D left panel). Similar results were obtained 24 hours after the chemotaxis assay (Figure 2E). These results suggest that mDia1 in DCs is indispensable for migration into the extracellular matrix protein-enriched area. We further evaluated the directional migration of BMDCs using TAXIScan and found that migration toward a gradient of the chemokine CCL21 was impaired by mDia1 deficiency in BMDCs (Figure 2F).

DC adhesion to FN was partially impaired by mDia1 deficiency

The interaction of DCs with extracellular matrix proteins, such as FN, is essential for their migration and formation of adhesion with integrins.[29] We evaluated localization of mDia1 in DCs and the effect of the deficiency of mDia1 on morphology and adhesions of BMDCs. We incubated BMDCs on plates coated with FN for 30 minutes and stained them with Alexa Fluor 488–labeled phalloidin and nonconjugated mDia1 Ab, followed by Alexa Fluor 546 goat anti–mouse IgG. Microscopic examination revealed that endogenous mDia1 was localized in the cytoplasm diffusely, and around the leading edge of B6 BMDCs strongly, and this localization was abolished in mDia1⁻/⁻ BMDCs (Figure 3A).

We then evaluated the morphology and adhesion of BMDCs. We incubated BMDCs for 30 minutes, 4 hours, and 18 hours, and stained them with Alexa Fluor 488–labeled phalloidin and nonconjugated mDia1 Ab, followed by Alexa Fluor 546 goat anti–mouse IgG. Most B6 DCs exhibited membrane protrusions at 30 minutes after incubation. The cells spread out 4 hours after incubation, and stress fibers were clearly formed 18 hours after cultivation (Figure 3B). In contrast, almost all mDia1⁻/⁻ BMDCs maintained their round shape without the formation of distinct membrane protrusions, but with distinct filopodia formation 30 minutes after incubation; and this apparent filopodia formation was still visible 4 hours, and even 18 hours after incubation (Figure 3B). To further evaluate podosome/focal adhesion formation, BMDCs were stained with Alexa Fluor 488–labeled phalloidin and nonconjugated vinculin Ab 4 hours after incubation, followed by Alexa Fluor 546 goat anti–mouse IgG. Although adhesion structures were detected in both B6 BMDCs and mDia1⁻/⁻ BMDCs (supplemental Figure 3A), the frequencies of cells with podosome and focal adhesion formation were significantly lower in mDia1-deficient cells (podosome formation: 61.3% ± 4.3% vs 52.9% ± 2.6%; focal adhesion:

Figure 3. mDia localization in DCs and characterization of cell morphology and adhesion in mDia1^{-/-} BMDCs. (A) mDia1 expression in DCs. B6 and mDia1^{-/-} BMDCs were incubated on FN-coated coverslips for 16 hours and stained with phalloidin and mDia1 Ab to reveal F-actin (green) and mDia1 (red). The cell nucleus was detected using 4,6-diamidino-2-phenylindole staining (blue). Bar represents 10 μm. (B) B6 and mDia1^{-/-} BMDCs incubated on FN-coated coverslips for 30 minutes, 4 hours, and 18 hours were stained with phalloidin; immunofluorescent images are shown. Open and closed arrowheads indicate membrane protrusion/lamellipodia and filopodia, respectively. (C) Morphology of BMDCs. B6 and mDia1^{-/-}BMDCs were incubated on coverslips coated with or without FN for 18 hours, and the major/minor axis ratio of BMDCs was measured. (D) Cell adhesion. B6 and mDia1^{-/-} BMDCs were labeled with CFSE and incubated in a 96-well-plate coated with or without FN for 45 minutes. The percentage of adherent BMDCs was measured using a fluorometer. Data are mean ± SD of 3 independent experiments. *$P < .05$ vs corresponding B6 mice.
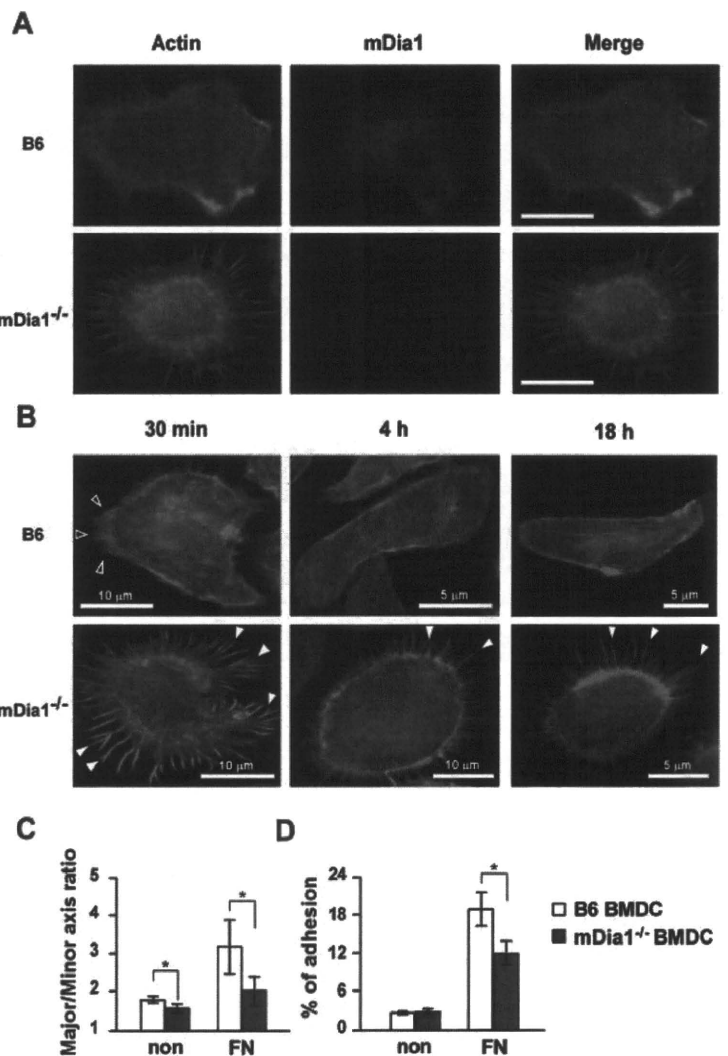
62.9% ± 3.1% vs 44.1% ± 3.1%; for B6 vs mDia1^{-/-} BMDCs, respectively; data presented as average ± SEM from 5 independent experiments, with 20 cells from each group evaluated). We then examined the surface expression levels of integrins and adhesion molecules, such as CD11a (LFA-1), CD11c, CD54 (ICAM-1), CD62L (L-selectin), and CD11b, and found that expression levels of these molecules were comparable between B6 BMDCs and mDia1^{-/-} BMDCs (supplemental Figure 3B). Lastly, we evaluated the cell polarity of BMDCs exposed for 30 minutes to CCL21 chemokine by staining with F-actin (supplemental Figure 3C). A chemokine gradient induced cell spreading of both B6 and mDia1^{-/-} BMDCs with a visible leading edge (supplemental Figure 3C). We evaluated the cell polarity and cell spreading by scoring BMDCs for polarized accumulation of actin[30] and evaluated the major/minor axis ratio. Both the cell polarity and cell spreading of mDia1^{-/-} BMDCs were less prominent than those of B6 BMDCs (supplemental Figure 3D-E). These results were consistent with the previous finding that the mean velocity of BMDCs to CCL21 was partially attenuated by mDia1 deficiency in a TAXIScan assay (Figure 2F).

We further evaluated the major/minor axes of BMDCs as indicators of cell polarity and protrusion after the BMDCs had been incubated on the coverslips for 16 hours. This parameter was significantly lower in mDia1^{-/-} BMDCs than in B6 BMDCs (Figure 3C). We next assessed the adhesion of BMDCs after a

45-minute incubation period. The incidence of adhesion of BMDCs to the plates, indicated as a percentage, was higher when the plate was coated with FN, and the incidence of adhesion was significantly higher in B6 BMDCs than in mDia1^{-/-} BMDCs (Figure 3D). These results suggest that mDia1 is an essential factor for the adhesion of DCs to FN, as well as for the establishment of cell polarity.

mDia1 deficiency in DCs impairs DC interaction with T cells

T-cell activation and differentiation require sustained interaction with DCs via integrins.[5] To investigate whether mDia1 deficiency in DCs impairs their interaction with T cells, we performed 3-dimensional live-imaging of DCs using 2-photon microscopy. To avoid environmental interference resulting from mDia1 deficiency in cells other than DCs, experiments were conducted using B6 mice as recipients for the transfer of B6 and mDia1^{-/-} BMDCs. The dynamics of DC behavior in draining popliteal LNs were evaluated through the injection of CFSE- or CMTPX-labeled BMDCs pretreated with LPS into the footpads of B6 mice (supplemental Video 1). The mean velocities, turning angles (ie, deviations from the previous orientation), and displacements (ie, distances between starting and ending positions) were comparable between B6 DCs and mDia1^{-/-} DCs (supplemental Figure 4A-C).

A

B6 OVA-pulsed BMDCs
OT-II CD4+ T cell

0 min   14 min   25 min

mDia1−/− OVA-pulsed BMDCs
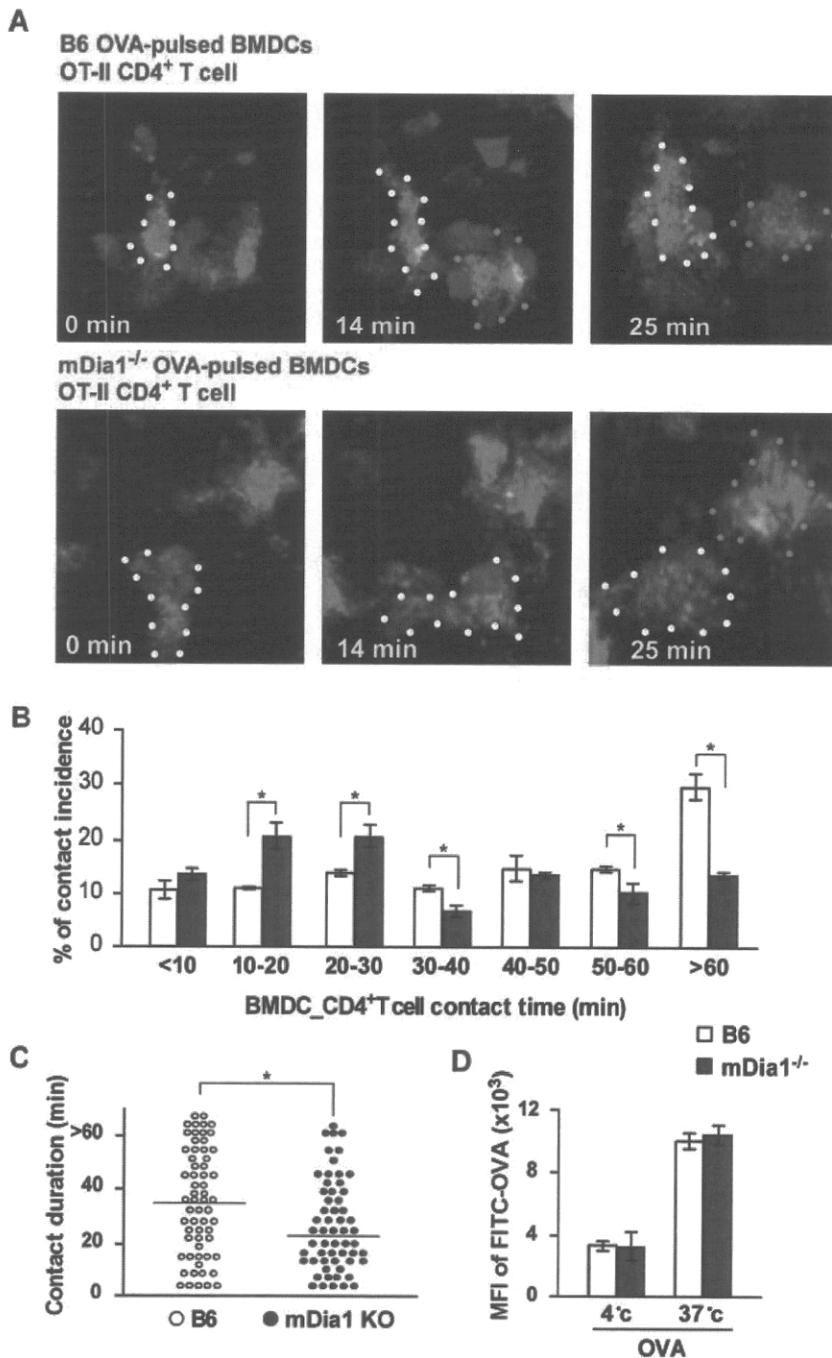**OT-II CD4+ T cell**

0 min   14 min   25 min

Figure 4. Impaired interaction with T cells resulting from mDia1 deficiency in DCs. (A) Time-lapse images of DC-T cell interaction ex vivo. OVA-pulsed CFSE-labeled B6 or mDia1−/− BMDCs were injected into mouse footpads, and CMTPX-labeled OT-II CD4+ T cells were intravenously administered. The popliteal LNs were collected and the DC–T-cell interaction was monitored using 2-photon microscopy; typical images at 0, 14, and 25 minutes are shown. White and red dots represent DCs. (B) Incidence of contact. Incidence of interactions of various durations between BMDCs and OT-II CD4+ T cells at 10-minute intervals. Data are mean ± SD and are representative of 3 experiments. (C) The overall duration of DC–T-cell interaction is shown. Data points represent individual durations. *P < .05 vs corresponding B6 mice. (D) Temperature-dependent activity of acquired antigens with FITC-OVA in MHC class II+ DCs of B6 mice and mDia1−/− mice. The activities of acquired antigens of DCs were observed by measuring the mean fluorescence intensity of ingested FITC at 4°C and 37°C for 45 minutes. Data are mean ± SD and are representative of 3 experiments.

B

C

D

☐ B6
■ mDia1−/−

We next evaluated DC–T-cell interaction in the LNs. T cells slow down their active migration and interact with DCs for up to several hours during the initial phase of T-cell priming.[31,32] BMDCs from B6 and mDia1−/− mice were pulsed with or without OVA, pretreated with LPS, labeled with CFSE, and injected into the footpads of mice. Twenty-four hours later, we intravenously transferred CMTPX-labeled CD4+ OT-II T cells, whose T-cell receptors specifically recognize OVA. An additional 2 hours later, we measured the duration of contacts formed between DCs and T cells in popliteal LNs during a 90-minute period of observation using 2-photon microscopy (supplemental Videos 2-3). The addition of OVA induced long-lasting contacts between B6 DCs and OT-II T cells; the length of these contacts was attenuated by mDia1 deficiency in DCs (Figure 4A-B). Our measurement of the dura-

tions of DC–T-cell conjugations revealed that mDia1−/− DCs exhibited higher rates of shorter-duration contacts, but lower rates of longer-duration contacts, than B6 DCs did (Figure 4B). Consistent with this, the overall mean duration of individual DC–T-cell interactions was shorter in mDia1−/− DCs than in B6 DCs (Figure 4C). We also evaluated whether the impaired T-cell–DC interaction brought about by mDia1 deficiency was not merely the result of impaired antigen acquisition by mDia1 BMDCs. The activity of temperature-dependent antigen acquisition of DCs was assessed by measuring FITC-labeled OVA in the cells using flow cytometry, and it was found that the activity levels were comparable between B6 and mDia1−/− mice (Figure 4D). Taken together, these results indicate that mDia1 expression in DCs is required to maintain sustained interactions with T cells.

Figure 5. Impaired T cell-stimulatory capacity of DCs resulting from mDia1 deficiency. (A-B) Alloreactive CD4+ T cells were purified from BALB/c mice and stimulated with or without B6 or mDia1−/− BMDCs in 200 μL of cRPMI for 72 hours. The numbers of each cell subset are shown in the figure. 3H-Thymidine incorporation in triplicate wells as an indicator of T-cell proliferation (A) and levels of IFN-γ in the culture supernatant (B) were measured. (C-E) The expression levels of MHC class II (C), CD40 (D), and CD54 (ICAM-1) (E) of BMDCs at 24 hours and 48 hours. Data are mean ± SD and are representative of 3 independent experiments. *P < .05 vs corresponding B6 mice.
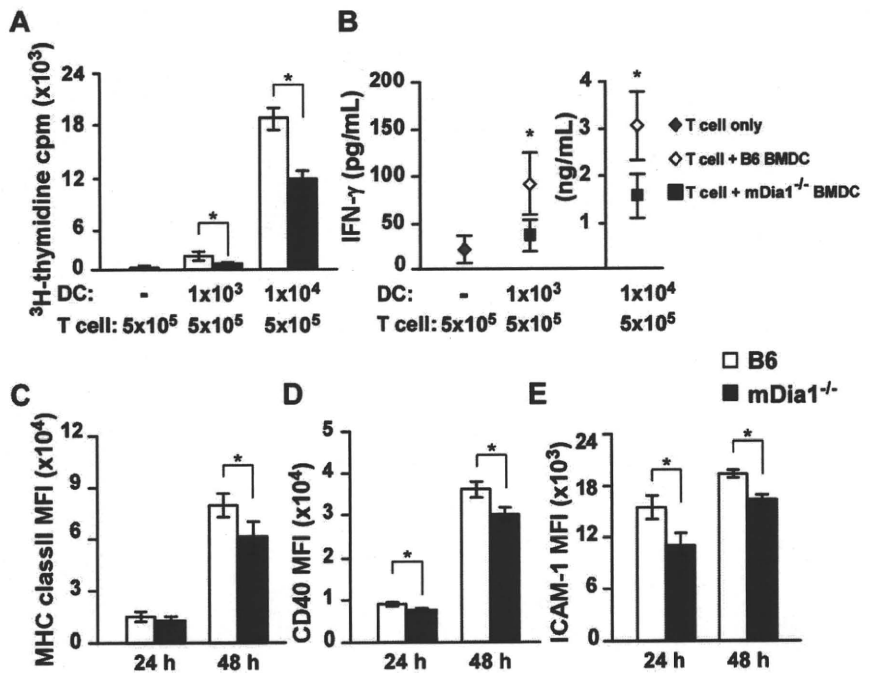
mDia1 deficiency attenuates T cell-stimulatory capacity of DCs in vitro

Based on the results we had thus far obtained, we sought to clarify whether mDia1 deficiency in DCs attenuated T cell-stimulatory capacity by MLR. Alloreactive CD4+ T cells were purified from BALB/c mice and stimulated with B6 or mDia1−/− BMDCs. Proliferation of T cells was lower in response to stimulation with mDia1−/− BMDCs than in response to stimulation with B6 BMDCs (Figure 5A). Consistently, levels of interferon-γ (IFN-γ) were lower in the supernatants of T-cell cultures stimulated with mDia1−/− BMDCs than in those stimulated with B6 BMDCs (Figure 5B). We further examined the expression levels of MHC class II, CD40, and CD54 as indicators of DC maturation 24 and 48 hours after cultivation, and found that mean fluorescence intensities of all surface markers of mDia1−/− BMDCs were lower than those of B6 BMDCs 48 hours after cultivation (Figure 5C-E). We assume that DCs undergo a further maturation on sustained interaction with T cells in an mDia1-dependent manner; therefore, mDia1 deficiency in DCs leads to impaired T-cell–stimulatory capacity in MLR.

Priming of T cells is reduced by mDia1 deficiency in vivo

Based on these results, we hypothesized that mDia1 deficiency in DCs leads to the attenuation of T-cell priming in vivo. We immunized B6 and mDia1−/− mice with OVA emulsified in CFA and transferred CFSE-labeled OT-II CD4+ T cells intravenously. Forty-eight hours later, draining popliteal and inguinal LN cells were dissociated, and dividing cells were measured with flow cytometry (Figure 6A-B). The numbers of total and dividing OT-II CD4+ T cells per draining LNs were significantly attenuated in mDia1−/− mice compared with B6 mice (Figure 6C). We also examined nondraining axillary LN cells for comparison purposes and found that the frequencies of CFSE+ OT-II CD4+ T cells to total cells were comparable in mDia1−/− and B6 mice (supplemental Figure 5). Cells in the process of division were not detected (supplemental Figure 5). In addition, the numbers of activated CD69+ CFSE+ cells and the relative amounts of IFN-γ mRNA

were lower in the draining LNs of mDia1−/− mice than in those of B6 mice (Figure 6D-E).

We next repeated the experiments using OT-I CD8+ T cells instead of OT-II CD4+ T cells, to evaluate the capacity of DCs to stimulate CD8+ T cells. Like that of OT-II CD4+ T cells, stimulation of OT-I CD8 T-cell proliferation was impaired by mDia1 deficiency in DCs (Figure 6F). These findings indicate that DCs require mDia1 to prime both CD4+ and CD8+ T cells in vivo.

Finally, we evaluated the impact of mDia1 deficiency in DCs on immune responses using a DTH model. B6 and mDia1−/− mice were subcutaneously sensitized with OVA in CFA in the front footpads and challenged with OVA in CFA in the hind footpads. Mice not subjected to OVA sensitization were used as a negative control. The hind footpad swelling change during the 48 hours after challenge was attenuated in mDia1−/− mice compared with B6 mice (Figure 6G), providing further evidence that mDia1 is critical for the T-cell priming ability of DCs in vivo. To avoid environmental interference resulting from mDia1 deficiency in cells other than DCs, we transferred B6 or mDia1−/− BMDCs pulsed with OVA into the front footpads and challenged the mice with OVA in CFA into the hind footpads. Mice injected with B6 BMDCs that had not been pulsed with OVA during sensitization were used as a negative control. The footpad thickness change was almost entirely abolished by mDia1 deficiency in DCs (Figure 6H). Thus, mDia1 in DCs is critical for the initiation of DTH response via T-cell priming in vivo.

Discussion

The role of mDia1 in the reorganization of the DC cytoskeleton has not yet been fully studied. In this report, we demonstrated that the number and maturation of DC subsets in the LNs, spleen, and the skin in the steady state, the development and maturation of BMDCs in vitro, and the motility of BMDCs in the LNs were not affected by mDia1 deficiency. However, DCs from mDia1−/− mice exhibited impaired transmigration of LCs through transwells with small pore

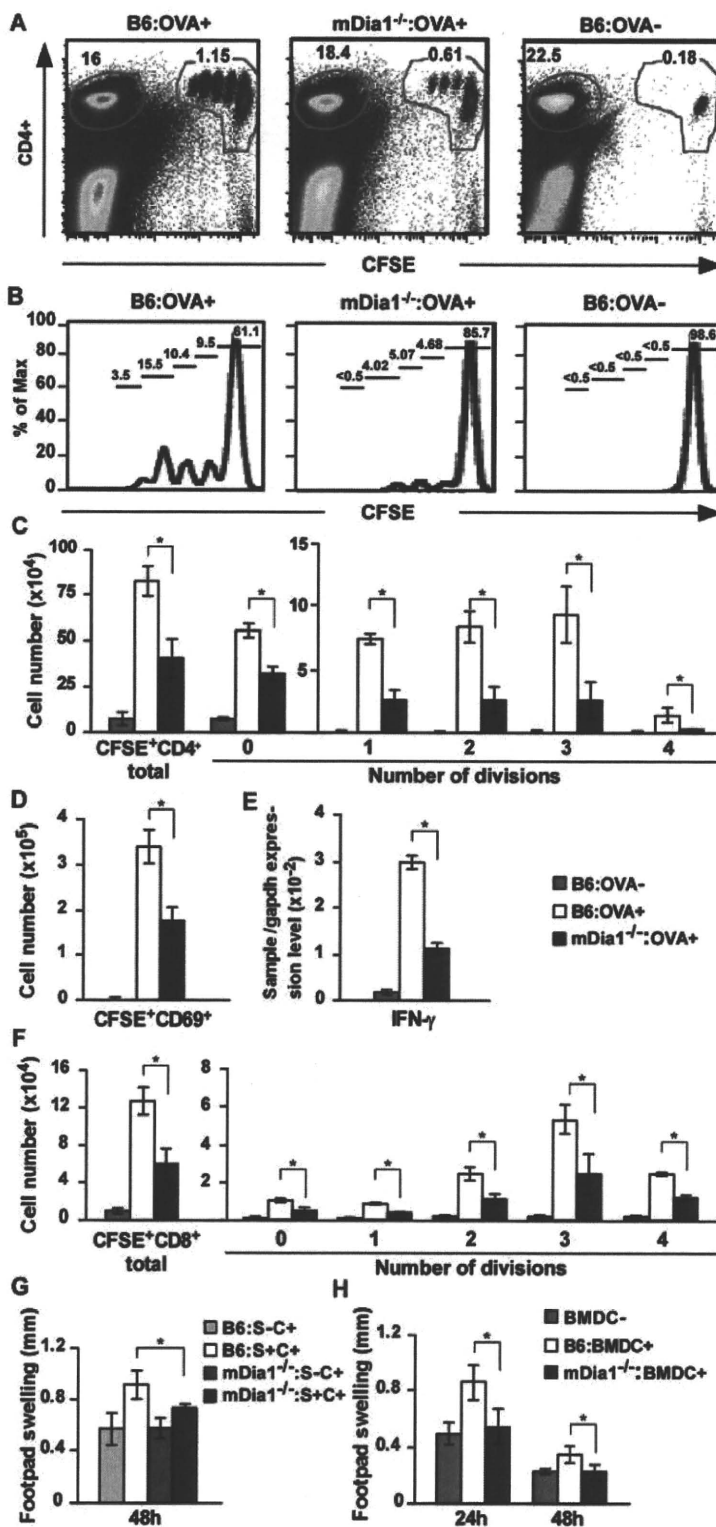**Figure 6. Attenuated CD4+ and CD8+ T-cell stimulation in mDia1−/− BMDCs.** (A-D) OT-II CD4+ T-cell stimulation by DCs. B6 and mDia1−/− mice were injected with CFA in the presence or absence of OVA, and CFSE-labeled OT-II CD4+ T cells were transferred intravenously. Forty-eight hours later, skin-draining popliteal and inguinal LN cells were collected and stained with CD4. Flow cytometry profiles (A), histograms of CFSE+ CD4+ cells (B), the numbers of CD4+ T cells per draining LNs in each division (C), and the numbers of CD69+ activated T cells (D) per draining LNs are shown. The numbers indicated in A are the ratio (%) of CD4+ CFSE+ cells (right) and CD4+ CFSE− cells to total cells. The numbers indicated in panel B are the ratio of each fraction to CD4+ CFSE+ cells. (E) IFN-γ mRNA expression was evaluated through quantitative reverse-transcribed polymerase chain reaction analysis. (F) OT-I CD8+ T-cell stimulation by DCs. CFSE-labeled OT-I CD8+ T cells were transferred intravenously to mice that had been pretreated as described in panels A to E, and the distribution of cell numbers in draining LNs is shown. (G) DTH induced by injection with OVA plus CFA. B6 and mDia1−/− mice were sensitized with OVA in CFA subcutaneously at the front footpads and challenged with OVA in CFA in the hind footpads. B6 and mDia1−/− mice that had not received OVA sensitization were used as negative controls. Footpad thickness change over 48 hours is shown. S indicates sensitization; and C, challenge. (H) DTH induced by OVA-pulsed BMDCs. We injected B6 or mDia1−/− BMDCs pulsed with (BMDC+) or without (BMDC−) OVA into the front footpads and challenged the mice by injecting OVA in CFA into the hind footpads. Administration of B6 BMDCs not pulsed with OVA during sensitization was used as a negative control. Footpad swelling data over 24 hours and 48 hours after challenge with OVA in CFA are shown. Data are mean ± SD and are representative of 3 independent experiments with similar results.

size, directional migration toward a chemokine gradient, cell adhesion to FN, and interaction with T cells. Consistent with this, the CD4+ and CD8+ T-cell–stimulating capacity of DCs, as well as their OVA-induced DTH response in vivo, were attenuated as a result of mDia1 deficiency. The results herein demonstrate the involvement of mDia1 at each step of DC functioning, as well as the importance of actin cytoskeletal reorganization and cognate interaction through mDia1 in DCs.

Cell migration is frequently described as a multistep cycle. F-actin polymerization at the cell surface induces a membrane protrusion, which is subsequently anchored to the extracellular matrix by integrins, which couple with the cytoskeleton and transduce the internal force via the actin cytoskeletal network.[33,34] Although motility in the LNs and invasion into the extracellular matrix–rich area remained mostly intact in mDia1−/− BMDCs, the transmigration to CCL21 through transwells with small pore size,

migration of mDia1$^{-/-}$ BMDCs across the Matrigel-coated transwell, and directional migration to chemokine on TAXIScan were all impaired. In addition, cell spreading and membrane protrusion were attenuated in mDia1$^{-/-}$ BMDCs. These findings probably explain the in vivo finding that FITC-induced cutaneous DC migration from the skin to the draining LNs was impaired. Using rat C6 glioma cells, Yamana et al demonstrated that mDia1 is required for cell polarization, cell focal adhesion turnover, and microtubule stabilization, possibly through the collaboration with Rac and Cdc42.[14] Therefore, the role of Rac/Cdc42 in mDia1$^{-/-}$ DCs in cell spreading and adhesion is worthy of future study.

Recent findings have suggested that integrins are essential for crossing the endothelial or epithelial lining, but not for migration of DCs in 3-dimensional environments.[35] Instead, these cells migrate solely by the force of actin-network expansion, which promotes the protrusive flow of the leading edge. In addition, the dynamics of DC behavior were not affected by deficiency of mDia1 in LNs in the steady state, which implies that mDia1 is not necessary for DCs to perform "amoeboid movement."[36] On the other hand, the invasive migration through the Matrigel and the directional migration to a chemokine gradient were attenuated in mDia1$^{-/-}$ BMDCs. Therefore, mDia1 appears indispensable for invasive movement in the extracellular matrix-rich area and directional movements toward a chemokine gradient, which depends on cell polarity (at least in part).

It is notable that behavior similar to that of mDia1$^{-/-}$ DCs, such as decreased adhesion and defects in T cell-stimulating capacity, has been observed in WASP$^{-/-}$ DCs.[37-39] Yet the impairments in maturation and chemotaxis and the dislocalization of DCs in the LNs that were observed in WASP$^{-/-}$ DCs[38] were not observed in mDia1$^{-/-}$ DCs. Yet although WASP-deficient DCs form abnormal lamellipodia resulting in hyperelongated morphology,[40] mDia1$^{-/-}$ DCs exhibit a rather round morphology without stress fiber formation. Collectively, these results suggest that the 2 actin-nucleating systems work together to enable the functions of DCs and that the lack of either cannot be compensated for by the other.

Given that the mDia family plays an elemental role in the actin filament dynamics in DCs, it is surprising that mDia1$^{-/-}$ DCs

exhibited relatively mild and limited dysfunction. We[16] and others[17] have previously found only partial impairment of T-cell trafficking in mDia1$^{-/-}$ mice. This may be partly explained by the fact that the roles of the other mDia isoforms, mDia2 and mDia3, overlap somewhat with those of mDia1.[9] In addition, we demonstrated that the mDia2 expression level in mDia1$^{-/-}$ DCs was elevated, which suggests that mDia2 might be induced to compensate for the deficiency of mDia1. Intriguingly, although mDia1 deficiency appears to cause only partial impairment of DC functioning at each step, its overall impact on the DTH response in DCs was nearly complete. The roles of mDia2 and mDia3 in DCs, as well as the role of WASP in relation to mDia1, are important topics for future study.

Acknowledgments

Authorship

Contribution: H.T. performed experiments, analyzed data, and wrote the paper; G.E., K.I., T.H., S. Nakajima, C.S.M., A.O., T.I., M.T., T.W., Y.M., S. Narumiya, and T.O. analyzed and discussed the data; and K.K. designed the research, analyzed the data, and cowrote the paper.

Conflict-of-interest disclosure: The authors declare no competing financial interests.

Correspondence: Kenji Kabashima, Department of Dermatology, Kyoto University Graduate School of Medicine, Yoshida, Sakyo-ku, Kyoto 606-8501, Japan; e-mail: kaba@kuhp.kyoto-u.ac.jp.

References

1. Banchereau J, Steinman RM. Dendritic cells and the control of immunity. *Nature.* 1998;392(6673):245-252.

2. Alvarez D, Vollmann EH, von Andrian UH. Mechanisms and consequences of dendritic cell migration. *Immunity.* 2008;29(3):325-342.

3. Randolph GJ, Angeli V, Swartz MA. Dendritic-cell trafficking to lymph nodes through lymphatic vessels. *Nat Rev Immunol.* 2005;5(8):617-628.

4. Kabashima K, Shiraishi N, Sugita K, et al. CXCL12-CXCR4 engagement is required for migration of cutaneous dendritic cells. *Am J Pathol.* 2007;171(4):1249-1257.

5. Dustin ML. T-cell activation through immunological synapses and kinapses. *Immunol Rev.* 2008;221:77-89.

6. Ridley AJ, Schwartz MA, Burridge K, et al. Cell migration: integrating signals from front to back. *Science.* 2003;302(5651):1704-1709.

7. Calle Y, Burns S, Thrasher AJ, Jones GE. The leukocyte podosome. *Eur J Cell Biol.* 2006;85(3):151-157.

8. Pulecio J, Tagliani E, Scholer A, et al. Expression of Wiskott-Aldrich syndrome protein in dendritic cells regulates synapse formation and activation of naive CD8+ T cells. *J Immunol.* 2008;181(2):1135-1142.

9. Faix J, Grosse R. Staying in shape with formins. *Dev Cell.* 2006;10(6):693-706.

10. Thrasher AJWA Sp in immune-system organization and function. *Nat Rev Immunol.* 2002;2(9):635-646.

11. Ochs HD, Thrasher AJ. The Wiskott-Aldrich syndrome. *J Allergy Clin Immunol.* 2006;117(4):725-738; quiz 739.

12. Le Clainche C, Carlier MF. Regulation of actin assembly associated with protrusion and adhesion in cell migration. *Physiol Rev.* 2008;88(2):489-513.

13. Goode BL, Eck MJ. Mechanism and function of formins in the control of actin assembly. *Annu Rev Biochem.* 2007;76:593-627.

14. Yamana N, Arakawa Y, Nishino T, et al. The Rho-mDia1 pathway regulates cell polarity and focal adhesion turnover in migrating cells through mobilizing Apc and c-Src. *Mol Cell Biol.* 2006;26(18):6844-6858.

15. Narumiya S, Tanji M, Ishizaki T. Rho signaling, ROCK and mDia1, in transformation, metastasis and invasion. *Cancer Metastasis Rev.* 2009;28(1):65-76.

16. Sakata D, Taniguchi H, Yasuda S, et al. Impaired T lymphocyte trafficking in mice deficient in an actin-nucleating protein, mDia1. *J Exp Med.* 2007;204(9):2031-2038.

17. Eisenmann KM, West RA, Hildebrand D, et al. T cell responses in mammalian diaphanous-related formin mDia1 knock-out mice. *J Biol Chem.* 2007;282(34):25152-25158.

18. Kobayashi M, Azuma E, Ido M, et al. A pivotal role of Rho GTPase in the regulation of morphology and function of dendritic cells. *J Immunol.* 2001;167(7):3585-3591.

19. Kabashima K, Murata T, Tanaka H, et al. Thromboxane A2 modulates interaction of dendritic cells and T cells and regulates acquired immunity. *Nat Immunol.* 2003;4(7):694-701.

20. Kabashima K, Sugita K, Shiraishi N, Tamamura H, Fujii N, Tokura Y. CXCR4 engagement promotes dendritic cell survival and maturation. *Biochem Biophys Res Commun.* 2007;361(4):1012-1016.

21. Yoshiki R, Kabashima K, Sugita K, Atarashi K, Shimauchi T, Tokura Y. IL-10-producing Langerhans cells and regulatory T cells are responsible for depressed contact hypersensitivity in grafted skin. *J Invest Dermatol.* 2009;129(3):705-713.

22. Nitta N, Tsuchiya T, Yamauchi A, Tamatani T, Kanegasaki S. Quantitative analysis of eosinophil chemotaxis tracked using a novel optical device: TAXIScan. *J Immunol Methods.* 2007;320(1):155-163.

23. Miller MJ, Wei SH, Parker I, Cahalan MD. Two-photon imaging of lymphocyte motility and antigen response in intact lymph node. *Science.* 2002;296(5574):1869-1873.

24. Livak KJ, Schmittgen TD. Analysis of relative gene expression data using real-time quantitative PCR and the 2(-Delta Delta C(T)) Method. *Methods.* 2001;25(4):402-408.

25. Randolph GJ, Inaba K, Robbiani DF, Steinman RM, Muller WA. Differentiation of phagocytic monocytes into lymph node dendritic cells in vivo. *Immunity.* 1999;11(6):753-761.

26. Sato K, Imai Y, Irimura T. Contribution of dermal macrophage trafficking in the sensitization phase of contact hypersensitivity. *J Immunol.* 1998; 161(12):6835-6844.

27. Kabashima K, Sakata D, Nagamachi M, Miyachi Y, Inaba K, Narumiya S. Prostaglandin E2-EP4 signaling initiates skin immune responses by promoting migration and maturation of Langerhans cells. *Nat Med.* 2003;9(6):744-749.

28. Sanz-Moreno V, Gadea G, Ahn J, et al. Rac activation and inactivation control plasticity of tumor cell movement. *Cell.* 2008;135(3):510-523.

29. Pankov R, Yamada KM. Fibronectin at a glance. *J Cell Sci.* 2002;115(20):3861-3863.

30. Shimonaka M, Katagiri K, Nakayama T, et al. Rap1 translates chemokine signals to integrin activation, cell polarization, and motility across vascular endothelium under flow. *J Cell Biol.* 2003;161(2):417-427.

31. Mempel TR, Henrickson SE, Von Andrian UH. T-cell priming by dendritic cells in lymph nodes occurs in three distinct phases. *Nature.* 2004;427 (6970):154-159.

32. Hugues S, Fetler L, Bonifaz L, Helft J, Amblard F, Amigorena S. Distinct T cell dynamics in lymph nodes during the induction of tolerance and immunity. *Nat Immunol.* 2004;5(12):1235-1242.

33. Lauffenburger DA, Horwitz AF. Cell migration: a physically integrated molecular process. *Cell.* 1996;84(3):359-369.

34. Mitchison TJ, Cramer LP. Actin-based cell motility and cell locomotion. *Cell.* 1996;84(3):371-379.

35. Lammermann T, Bader BL, Monkley SJ, et al. Rapid leukocyte migration by integrin-independent flowing and squeezing. *Nature.* 2008;453(7191):51-55.

36. de Bruyn PPH. The amoeboid movement of the mammalian leukocyte in tissue culture. *Ant. Rec.* 1946;95:117-192.

37. Bouma G, Burns S, Thrasher AJ. Impaired T-cell priming in vivo resulting from dysfunction of WASp-deficient dendritic cells. *Blood.* 2007; 110(13):4278-4284.

38. Bouma G, Burns SO, Thrasher AJ. Wiskott-Aldrich syndrome: immunodeficiency resulting from defective cell migration and impaired immunostimulatory activation. *Immunobiology.* 2009; 214(9):778-790.

39. de Noronha S, Hardy S, Sinclair J, et al. Impaired dendritic-cell homing in vivo in the absence of Wiskott-Aldrich syndrome protein. *Blood.* 2005; 105(4):1590-1597.

40. Burns S, Thrasher AJ, Blundell MP, Machesky L, Jones GE. Configuration of human dendritic cell cytoskeleton by Rho GTPases, the WAS protein, and differentiation. *Blood.* 2001;98(4):1142-1149.

Letter to the Editor

Enhanced murine contact hypersensitivity by depletion of endogenous regulatory T cells in the sensitization phase

To the Editor,

Regulatory T cells (Treg) play essential roles in the regulation of immune responses [1]. Contact hypersensitivity (CHS) is a prototype of T-cell mediated delayed-type hypersensitivity reactions [2], mainly mediated by interferon (IFN)-γ producing type 1 helper T cells and cytotoxic T cells [3]. Transfer of exogenous Treg during the elicitation phase is known to suppress CHS in IL-10 [4] and CD39 dependent manners [5]. However, Foxp3, a master transcriptional factor and thus far the only reliable marker for Treg, exists intracellularly, hampering *ex vivo* isolation or *in vivo* depletion of endogenous Treg. Therefore, it remains largely unclear whether endogenous Treg mediate such suppressive roles *in vivo*.

Recently, we have developed Foxp3 reporter mice expressing human CD2/CD52 fusion protein on cell surfaces of Foxp3$^+$ Treg. In the Foxp3$^{hCD2/hCD52}$ mice, Treg can be depleted with a neutralizing ablative rat anti-human CD52 antibody (Ab), Campath-1G Ab [6]. Using this model, we reported that depletion of Treg in the elicitation phase of CHS prolonged inflammatory responses, indicating that endogenous Treg are critical for termination of CHS responses [6]. In this study, we evaluated the roles of endogenous Treg focusing on the sensitization phase of CHS.

Treatment of Campath-1G Ab (0.5 mg/body) depleted Treg by 70% 48 h later [6] and by 50% 1 day and 6 days later (Supplementary data, Fig. S1a and b). First, we evaluated the CHS reaction by depleting Treg during both the sensitization and elicitation phases. We administered control rat IgG Ab (Sigma–Aldrich) or Campath-1G Ab to Foxp3$^{hCD2/hCD52}$ mice, and sensitized mice with 25 μl of 0.5% (w/v) dinitrofluorobenzene (DNFB) (Nacalai Tesque, Kyoto, Japan) in acetone/olive oil (4/1) on shaved abdominal skin on the next day, and challenged the mice with 20 μl of 0.3% (w/v) DNFB in acetone/olive oil (4/1) on ear skin 5 days later. Treatment with Campath-1G Ab significantly enhanced an ear swelling responses compared with control Ab treatment (Fig. 1a), indicating that Treg depletion during both the sensitization and elicitation phases sustained CHS response. To evaluate the effect of Treg depletion during the sensitization phase, we elicited mice 21 days after Campath-1G Ab administration, when the numbers of Treg had completely recovered after Campath-1G Ab treatment (Supplementary data, Fig. S1b). Even then, mice treated with Campath-1G Ab showed a consistently enhanced ear swelling response compared with the control mice (Fig. 1b). Treatment with Campath-1G didn't cause enhancement of CHS in WT mice (Supplementary data, Fig. S2a), confirming the specificity on the effect of Campath1-G Ab. These results indicate that endogenous Treg play a suppressive role in the sensitization phase of CHS.

We next investigated the effect of Treg depletion on memory T cell induction in draining lymph nodes (dLNs). Axillary and inguinal LN cells were taken 5 days after DNFB sensitization, and stained with fluorescent-labeled CD4, CD8, CD44, and CD62L Abs (eBioscience, San Diego, CA, USA), and analyzed with FACSCanto II (BD Bioscience, San Diego, CA, USA) and FlowJo software (Tree Star, Ashland, OR, USA). The percentage and the number of both CD44$^+$ CD62L$^+$ central memory and CD44$^+$ CD62L-effector memory CD4 and CD8 T cells in the dLNs were significantly higher in mice with Campath-1G Ab (Fig. 1c and d). No such effects were observed in WT mice treated with Campath-1G Ab (Supplementary data, Fig. S2b). Furthermore, IFN-γ production in the supernatant of 1×10^6 LN cells of Campath-1G Ab-treated mice after cultivation for 72 h in 200 μl in 96-well-plates was significantly higher than that of control Ab-treated mice (Fig. 1e). These results suggest that endogenous Treg play a suppressive role in the sensitization phase of CHS by inhibiting the induction of memory T cells.

For the induction of memory T cells, dendritic cells (DCs) play crucial roles by presenting antigen to naïve T cells via MHC class II in combination with co-stimulatory molecules. It has been reported that the addition of exogenous Treg suppresses co-stimulatory molecule expressions on DCs *in vitro*. To investigate the inhibitory mechanism by which endogenous Treg inhibit memory T cell induction, we examined the effect of Treg depletion on the co-stimulatory molecule expression in DCs. We analyzed the expression levels of co-stimulatory molecules and MHC class II in CD11c^{low} MHC class II^{high} migrating DCs 5 days after DNFB sensitization. Mice treated with Campath-1G Ab showed significantly higher expression of CD86 and CD80 (Fig. 2a), while no significant differences were detected in CD40 and MHC class II expression. We also found that Treg depletion enhanced CD86 expression, but not fluorescein isothiocyanate (FITC)-induced cutaneous DC migration to dLNs (Supplementary data, Fig. S3). We further examined the localization of Treg and DC in skin dLNs by immunohistochemical analyses. Frozen sections of cervical LNs from C57BL/6 mice were stained with rat anti-Foxp3 Ab (eBioscience), followed by goat anti-rat Alexafluor 488 (Invitrogen), and then with Alexafluor 647-labeled rat anti-Langerin Ab (eBioscience). We found that numerous Treg localizing around DC (Fig. 2b). These results suggest the possibility that endogenous Treg contribute to the modulation of DC function in dLNs.

Finally, we investigated the effect of endogenous Treg on the naïve T cell activation. CD4$^+$ T cells were purified from skin dLNs of Foxp3$^{hCD2/hCD52}$ mice by negative selection using auto MACS (Miltenyi Biotech, Bergisch Gladbach, Germany). CD4$^+$ hCD2$^+$ Treg were depleted or not from purified CD4$^+$ T cells by FACSAria (BD Bioscience). Then, 4×10^4 CD4$^+$ hCD2$^-$ non-Treg subset with or without endogenous CD4$^+$ hCD2$^+$ Treg were stimulated with anti-CD3 Ab in round bottom 96 well plates for 72 h, and ^{3}H-thymidine was added for the last 12 h. Absence of Treg induced higher cell proliferation and IFN-γ production (Fig. 2c and d), suggesting that endogenous Treg suppress naïve T cell activation and proliferation.
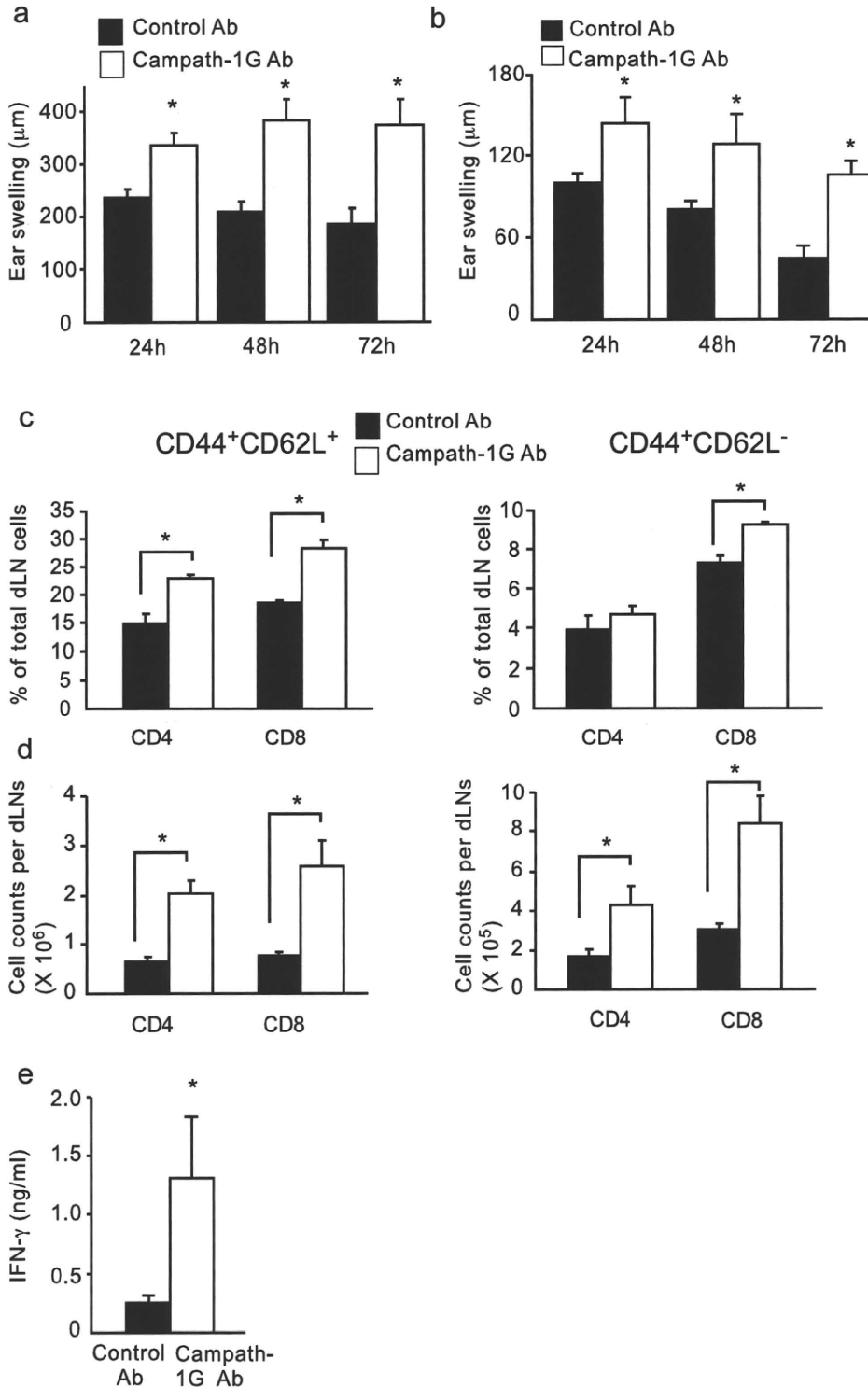
Fig. 1. Effect of Treg depletion during sensitization phase on CHS response. (a–e) Ear swelling by elicitation 5 days (a) or 20 days (b) after sensitization. The percentage (c) and the number (d) of memory T cells in dLNs 5 days after DNFB sensitization. (e) IFN-γ production in culture supernatant of dLN cells after 72 h culture. Data are presented as the mean ± SD and are a representative of three independent experiments with similar results. Statistical analyses were performed by Student's *t* test. *N* = 3. * *P* < 0.05.

Collectively, our results suggest that endogenous Treg play suppressive roles during the sensitization phase of CHS by down-modulating DC functions in the dLNs, which is consistent with previous studies that exogenously transferred Treg suppress DCs-mediated T cell activation [7–10], Further studies to reveal the precise molecular suppression mechanisms of endogenous Treg in CHS will help us to develop a new therapeutic strategy for undesired cutaneous immune responses.
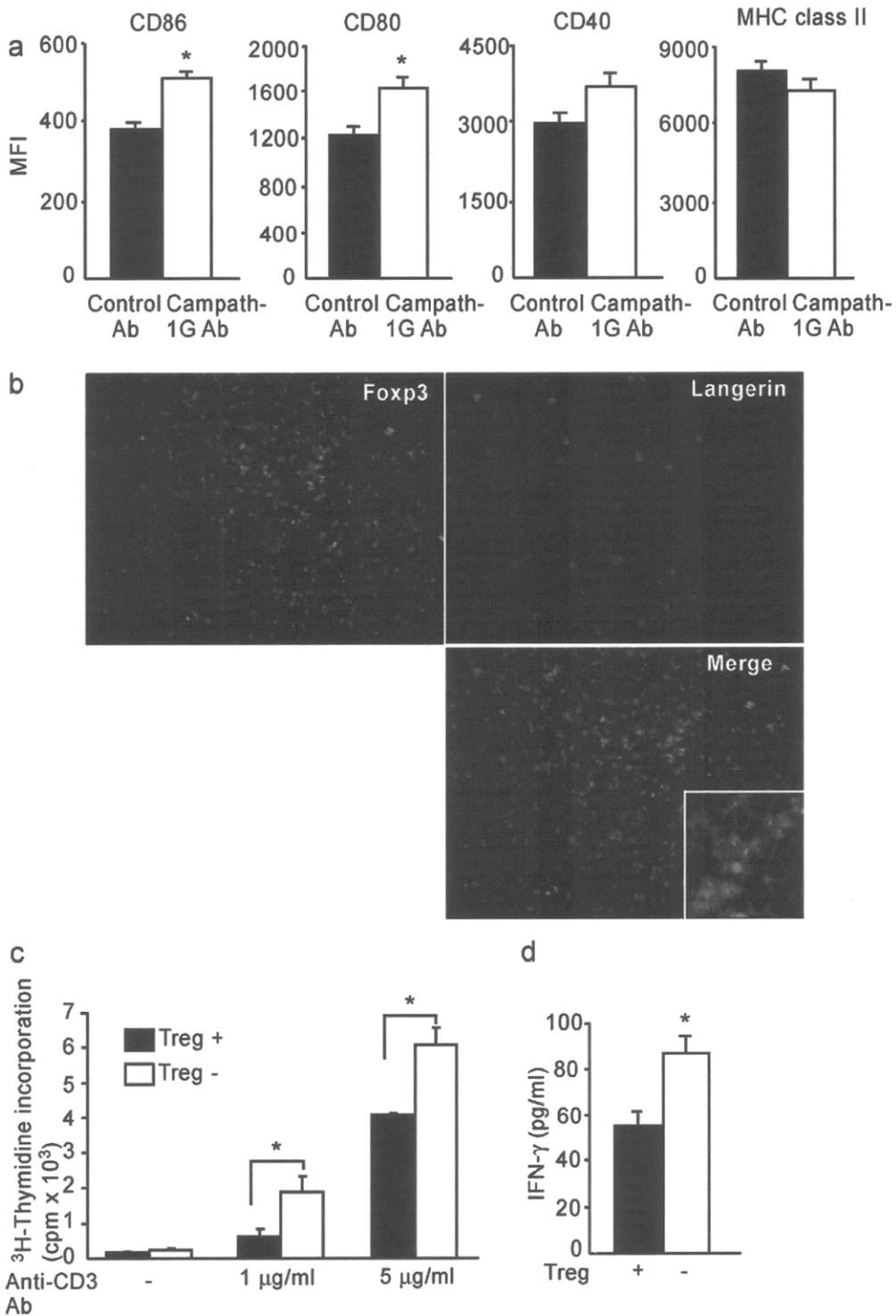
Fig. 2. Effect of Treg depletion on DC and T cell activation. (a) Co-stimulatory molecules expression levels on CD11c^{low}MHC classII^{high} DCs in dLNs after DNFB sensitization. (b) Colocalization of Foxp3$^+$ Treg and Langerin$^+$ DCs in LNs revealed by immunohistochemistry. (c) T cell proliferation and (d) IFN-γ production in culture supernatants stimulated with anti-CD3 Ab. Data are presented as the mean ± SD and are a representative of two independent experiments with similar results. $N = 3$. Statistical analyses were performed by Student's t test. *$P < 0.05$.

Acknowledgements

Appendix A. Supplementary data

Supplementary data associated with this article can be found, in the online version, at doi:10.1016/j.jdermsci.2010.11.001.

References

[1] Sakaguchi S, Yamaguchi T, Nomura T, Ono M. Regulatory T cells and immune tolerance. Cell 2008;133:775–87.

[2] Grabbe S, Schwarz T. Immunoregulatory mechanisms involved in elicitation of allergic contact hypersensitivity. Immunol Today 1998;19:37–44.

[3] Mori T, Kabashima K, Yoshiki R, Sugita K, Shiraishi N, Onoue A, et al. Cutaneous hypersensitivities to hapten are controlled by IFN-gamma-upregulated keratinocyte Th1 chemokines and IFN-gamma-downregulated langerhans cell Th2 chemokines. J Invest Dermatol 2008;128:1719–27.

[4] Ring S, Schafer SC, Mahnke K, Lehr HA, Enk AH. CD4+ CD25+ regulatory T cells suppress contact hypersensitivity reactions by blocking influx of effector T cells into inflamed tissue. Eur J Immunol 2006;36:2981–92.

[5] Ring S, Oliver SJ, Cronstein BN, Enk AH, Mahnke K. CD4+ CD25+ regulatory T cells suppress contact hypersensitivity reactions through a CD39, adenosine-dependent mechanism. J Allergy Clin Immunol 2009;123:1287–96. e1282.

[6] Tomura M, Honda T, Tanizaki H, Otsuka A, Egawa G, Tokura Y, et al. Activated regulatory T cells are the major T cell type emigrating from the skin during a cutaneous immune response in mice. J Clin Invest 2010;120(3):883–93.

[7] Onishi Y, Fehervari Z, Yamaguchi T, Sakaguchi S. Foxp3+ natural regulatory T cells preferentially form aggregates on dendritic cells in vitro and actively inhibit their maturation. Proc Natl Acad Sci USA 2008;105:10113–8.

[8] Schwarz A, Schwarz T. UVR-induced regulatory T cells switch antigen-presenting cells from a stimulatory to a regulatory phenotype. J Invest Dermatol 2010;130:1914–21.

[9] Tang Q, Adams JY, Tooley AJ, Bi M, Fife BT, Serra P, et al. Visualizing regulatory T cell control of autoimmune responses in nonobese diabetic mice. Nat Immunol 2006;7:83–92.

[10] Tadokoro CE, Shakhar G, Shen S, Ding Y, Lino AC, Maraver A, et al. Regulatory T cells inhibit stable contacts between CD4+ T cells and dendritic cells in vivo. J Exp Med 2006;203:505–11.

Tetsuya Honda*
Department of Dermatology, Kyoto University, Kyoto, Japan

Atsushi Otsuka
Department of Dermatology, Kyoto University, Kyoto, Japan

Hideaki Tanizaki
Department of Dermatology, Kyoto University, Kyoto, Japan

Yosuke Minegaki
Department of Dermatology, Kyoto University, Kyoto, Japan

Keisuke Nagao
Department of Dermatology, Keio University, Tokyo, Japan

Herman Waldmann
Sir William Dunn School of Pathology, Oxford, United Kingdom

Michio Tomura
Laboratory for Cell Function and Dynamics, Advanced Technology Development Center, Brain Science Institute, RIKEN, Wako, Japan

Shohei Hori
Research Unit for Immune Homeostasis, Research Center for Allergy and Immunology, RIKEN, Yokohama City, Japan

Yoshiki Miyachi
Department of Dermatology, Kyoto University, Kyoto, Japan

Kenji Kabashima*
Department of Dermatology, Kyoto University, Kyoto, Japan

*Corresponding authors at: Department of Dermatology, Kyoto University Graduate School of Medicine, Yoshida, Sakyo-ku, Kyoto 606-8501, Japan. Tel.: +81 75 753 9502, fax: +81 75 753 9500
E-mail address: hontetsu@kuhp.kyoto-u.ac.jp
kaba@kuhp.kyoto-u.ac.jp

20 August 2010
Available online xxx

Upregulation of Aquaporin-3 Is Involved in Keratinocyte Proliferation and Epidermal Hyperplasia

Kyoko Nakahigashi[1], Kenji Kabashima[1], Akihiko Ikoma[1], Alan S. Verkman[2], Yoshiki Miyachi[1] and Mariko Hara-Chikuma[1]

Aquaporin-3 (AQP3) is a water/glycerol-transporting protein expressed in keratinocytes of the epidermis. We previously showed that AQP3-mediated transport of water and glycerol is involved in keratinocyte migration and proliferation, respectively. However, the involvement of AQP3 in epidermal hyperplasia in skin diseases, such as atopic dermatitis (AD), is unknown. In this study, we found significantly increased AQP3 transcript and protein expression in the epidermis of human AD lesions. The upregulation of AQP3 expression in human keratinocytes by transfection with human AQP3 DNA plasmid was associated with increased cellular glycerol and ATP, as well as increased cell proliferation. Among several cytokines and chemokines produced in the skin, CCL17, which is highly expressed in AD, was found to be a strong inducer of AQP3 expression and enhanced keratinocyte proliferation. In mouse AD models, AQP3 was strongly overexpressed in the epidermis in wild-type mice. Epidermal hyperplasia was reduced in AQP3-deficient mice, with a decreased number of proliferating keratinocytes. These results suggest the involvement of AQP3 in epidermal hyperplasia by a mechanism involving upregulated AQP3 expression and consequent enhancement of keratinocyte proliferation.

INTRODUCTION

The aquaporins (AQPs, named AQP0–12) are a family of transmembrane channels that transport water, and in some cases small solutes such as glycerol (Carbrey and Agre, 2009; Verkman, 2009). AQP3 is one such water/glycerol-transporting protein, which is expressed in keratinocytes of the epidermis (Ma *et al.*, 2002). Our previous studies using AQP3 knockout mice and human keratinocytes showed that AQP3-mediated water and glycerol transport is involved in keratinocyte migration and proliferation, respectively, which were implicated to have important roles in cutaneous wound healing and tumorigenesis (Hara-Chikuma and Verkman, 2008a, b). We have also shown that AQP3 deficiency has little effect on differentiation markers in human keratinocytes, suggesting that AQP3 is not involved in keratinocyte differentiation (Hara-Chikuma *et al.*, 2009). Previous conflicting studies had suggested that AQP3 is involved in early differentiation, but not in proliferation, of keratinocytes (Zheng and Bollag, 2003; Bollag *et al.*, 2007).

The development and maintenance of the mature epidermis rely on balanced keratinocyte proliferation and terminal differentiation. Hyperproliferation and disturbed differentiation are associated with certain pathological conditions, such as atopic dermatitis (AD), ichthyosis, and psoriasis (Fuchs and Raghavan, 2002; Jensen *et al.*, 2004). With regard to keratinocyte proliferation, multiple studies have shown that several growth factors and cytokines, including tumor necrosis factor-α (TNF-α), IFN-γ, IL-1, and GM-CSF, are involved in the growth of keratinocyte in skin disorders, such as epidermal barrier disruption and wound healing (Wood *et al.*, 1992; Segre, 2006; Barrientos *et al.*, 2008). Recent studies have revealed that both IL-21 and IL-23 mediate keratinocyte proliferation and epidermal hyperplasia, which was found to be implicated in the pathogenesis of psoriasis (Chan *et al.*, 2006; Caruso *et al.*, 2009).

The aim of this study was to investigate the hypothesis that AQP3 upregulation is involved in keratinocyte proliferation and epidermal hyperplasia in skin disorders. Motivated by the observation that AQP3 expression was increased in the AD skin (Olsson *et al.*, 2006), we used human keratinocytes and murine AD models in AQP3-null mice. We found that upregulation of AQP3 enhanced proliferation of human keratinocytes, which was involved in epidermal hyperplasia during AD development. Our data suggest that AQP3 inhibition by topical agents may be beneficial for the treatment of epidermal hyperplasia in AD.

RESULTS

Increased epidermal AQP3 expression in human AD

A previous report showed increased AQP3 transcript expression in the whole skin affected by atopic eczema (Olsson

[1]*Department of Dermatology, Graduate School of Medicine, Kyoto University, Kyoto, Japan and* [2]*Department of Medicine and Physiology, University of California, San Francisco, San Francisco, California, USA*

Correspondence: Mariko Hara-Chikuma, Department of Dermatology, Graduate School of Medicine, Kyoto University, 54, Kawahara-cho, Shogoin, Sakyo-ku, Kyoto 606-8507, Japan. E-mail: haramari@kuhp.kyoto-u.ac.jp
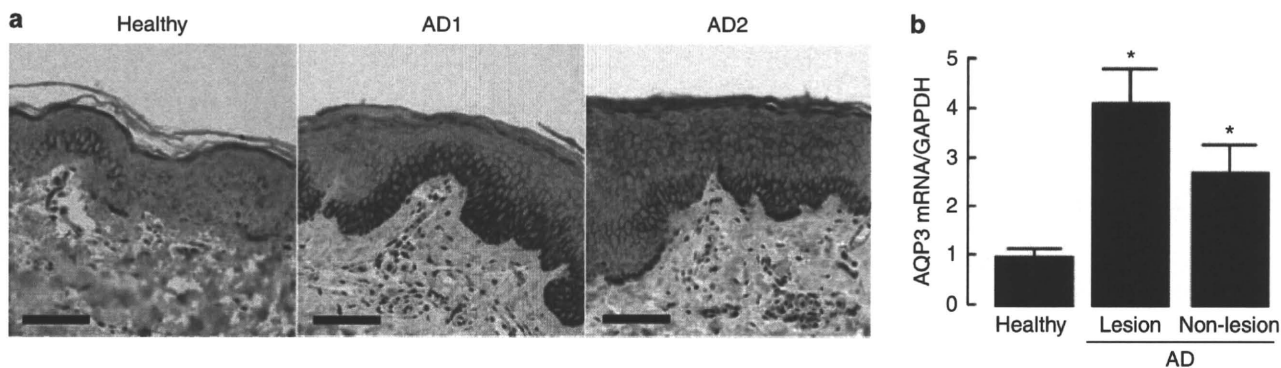
Figure 1. AQP3 expression in the epidermis of AD lesions and healthy subjects. (a) Skin specimens were immunostained with anti-AQP3. Left, healthy subject; right, lesion from AD patients. Bar = 50 µm. (b) AQP3 mRNA expression in the epidermis from AD patients (lesion, $n = 7$; non-lesion, $n = 4$) and healthy subjects ($n = 6$) by quantitative RT-PCR. Data are expressed as AQP3/GAPDH ratio (mean ± SE). *$P < 0.01$. AD, atopic dermatitis; AQP, aquaporin; GAPDH, glyceraldehyde-3-phosphate dehydrogenase; RT-PCR, reverse transcription-PCR.

et al., 2006). To verify AQP3 protein expression in the epidermis of AD lesions, we performed immunostaining with anti-AQP3 antibody. Figure 1a shows remarkably greater AQP3 protein expression on the plasma membrane of keratinocytes in AD lesions than in the healthy epidermis. AQP3 was broadly distributed throughout the AD lesions. To quantify AQP3 transcript expression, we isolated the epidermis from the AD skin (lesion and non-lesion) and assayed AQP3 mRNA by quantitative reverse transcription-PCR. Figure 1b shows approximately four-fold increased AQP3 transcript expression in the epidermis of AD lesions versus controls.

Greater AQP3 expression enhances keratinocyte proliferation
We determined whether increased AQP3 expression could enhance keratinocyte proliferation. Normal human keratinocytes (NHKs) were transfected with either empty vector or plasmid expressing human AQP3. Figure 2a shows that transfection of AQP3 plasmid produced at least 3.2-fold increase in AQP3 mRNA. Immunoblot analysis showed an approximately six-fold increase in AQP3 protein expression, with the expected molecular size of 28 kDa (Figure 2a, right). Keratins 5 and 14, markers of basal proliferating cells, were significantly increased in AQP3-overexpressing NHKs compared with empty vector-transfected cells (Figure 2b). We found no significant differences in keratins 1 and 10, markers of early differentiation. Measurement of cell growth using the modified MTT assay showed that AQP3 upregulation enhanced cell growth (Figure 2c). We have previously proposed that AQP3-facilitated glycerol transport is an important determinant of keratinocyte proliferation and cellular ATP generation (Hara-Chikuma and Verkman, 2008a, b). Levels of cellular glycerol and ATP were increased in NHKs with upregulated AQP3 expression (Figure 2d and e). These findings show that increased AQP3 expression enhances keratinocyte proliferation.

CCL17 increases AQP3 expression in human keratinocytes
It has been reported that various Th1 and Th2 cytokines/chemokines are altered in the epidermis in AD, which are proposed to be involved in epidermal hyperplasia and AD pathogenesis (Novak *et al.*, 2003). We asked whether

cytokines/chemokines could affect AQP3 expression in keratinocytes during the development of AD. Human keratinocytes (HaCaT) were used in this study to examine the effect of cytokines/chemokines on AQP3 expression, because the expressions of cytokine/chemokine receptors are more stable in HaCaT than in NHKs. Cells were incubated with cytokines/chemokines for 2 days, and AQP3 expression was quantified by immunoblotting. We found that TARC (thymus and activation-regulated chemokine)/CCL17, a Th2 chemotactic chemokine, increased AQP3 expression (Figure 3a). TNF-α significantly decreased AQP3 expression, which is consistent with previous data in a human squamous cell carcinoma cell line (DJM-1) (Horie *et al.*, 2009). Figure 3b shows that CCL17 increased AQP3 expression in a dose-dependent manner.

CCL17 is produced by dendritic cells, T cells, and keratinocytes (Reiss *et al.*, 2001). It has been reported that stimulation with IFN-γ and TNF-α synergistically induced CCL17 production in HaCaT cells (Vestergaard *et al.*, 2000). To elucidate the mechanism of CCL17-facilitated AQP3 upregulation, HaCaT keratinocytes were incubated with TNF-α and INF-γ, and assayed for CCL17 and AQP3 mRNA expression. Figure 3c shows that addition of TNF-α/INF-γ increased intrinsic CCL17 in keratinocytes approximately nine-fold, without effect on AQP3 expression. In contrast, incubation with CCL17 increased AQP3 expression, whereas intrinsic CCL17 expression was not altered. These results suggest that exogenous CCL17 affects AQP3 expression.

We next studied whether exogenous CCL17 could affect cell signaling, resulting in increased AQP3 expression. Cells were treated with various cell signaling inhibitors following incubation with CCL17 for 1 day, after which AQP3 mRNA expression was assessed. Figure 3d shows that mitogen-activated protein kinase and protein kinase C inhibitors (U0126 and R03-2432) suppressed CCL17-facilitated AQP3 upregulation, suggesting the involvement of CCL17-dependent mitogen-activated protein kinase and/or protein kinase C cell signaling in increased AQP3 expression.

CCL17 enhances keratinocyte proliferation
We determined the effect of CCL17 on keratinocyte proliferation. HaCaT keratinocytes were starved for 1 day,
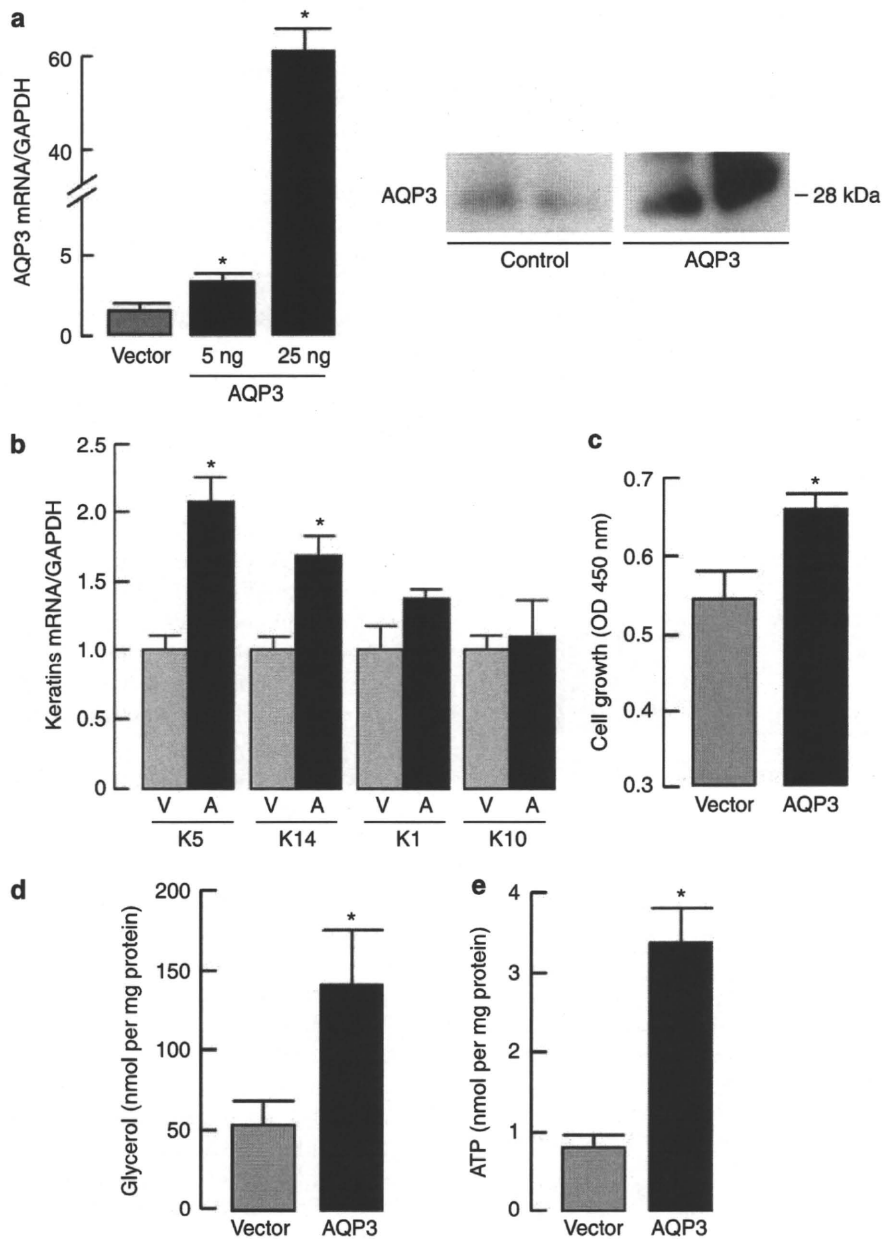
Figure 2. Effect of AQP3 upregulation in human keratinocytes. NHKs were transfected with empty vector (pCMV6-XL4) or plasmid expressing human AQP3 (5–25 ng per 8×10^3 cells). (**a**) (Left) The relative mRNA expression of AQP3/GAPDH (SE, $n = 4$–5, *$P < 0.01$). (Right) Immunoblot of cell homogenates with anti-AQP3 (15 μg protein per lane, 100 ng per 2×10^5 cells). (**b**) The relative mRNA expressions of keratins 5, 14, 1, and 10 in NHKs transfected with empty vector (V) or AQP3 plasmid (A). Data are expressed as keratins/GAPDH ratio (mean ± SE) ($n = 3$) *$P < 0.01$. (**c**) Cell proliferation was assessed by modified MTT assay (SE, $n = 5$, *$P < 0.01$, 5 ng per 8×10^3 cells). (**d**) Cellular glycerol content and (**e**) ATP content (SE, $n = 5$, *$P < 0.01$, 5 ng per 8×10^3 cells). AQP, aquaporin; GAPDH, glyceraldehyde-3-phosphate dehydrogenase; NHK, normal human keratinocyte.

and treated with CCL17 for 6 hours. AQP3 mRNA expression was increased 2.6-fold in CCL17-treated cells (Figure 4a, left). CCL17 also significantly increased the expressions of proliferation markers, keratins 5 and 14, but not those of differentiation markers, keratins 1 and 10 (Figure 4a, right). To examine the effect of CCL17 on cell growth, cells were treated with CCL17 for 2 days in the starved medium, after which cell proliferation was induced by replacing the medium with 0.1 or 2% fetal bovine serum. As shown in

Figure 4b, cell proliferation, assessed by BrdU incorporation, was significantly increased in CCL17-treated cells as compared with control cells. Finally, cell growth was assayed in controls and AQP3 knockdown keratinocytes to determine the involvement of AQP3 in CCL17-induced cell proliferation. Transfection of small-interfering RNA-AQP3 into HaCaT cells consistently reduced AQP3 mRNA expression by ~90% (9.1 ± 1.4% of controls). Figure 4c shows reduced CCL17-induced cell proliferation in AQP3 knockdown keratinocytes.